Thalassotitan atrox, a giant predatory mosasaurid (Squamata) from the upper Maastrichtian phosphates of Morocco

Nicholas Longrich, Nour-Eddine Jalil, Fatima Khaldoune, Oussama Khadiri Yazami, Xabier Pereda-Suberbiola, Nathalie Bardet

▶ **To cite this version:**

Nicholas Longrich, Nour-Eddine Jalil, Fatima Khaldoune, Oussama Khadiri Yazami, Xabier Pereda-Suberbiola, et al.. Thalassotitan atrox, a giant predatory mosasaurid (Squamata) from the upper Maastrichtian phosphates of Morocco. Cretaceous Research, 2022, 140, pp.105315. 10.1016/j.cretres.2022.105315 . mnhn-03861681

HAL Id: mnhn-03861681
https://mnhn.hal.science/mnhn-03861681v1

Submitted on 2 Nov 2023

HAL is a multi-disciplinary open access archive for the deposit and dissemination of scientific research documents, whether they are published or not. The documents may come from teaching and research institutions in France or abroad, or from public or private research centers.

L'archive ouverte pluridisciplinaire **HAL**, est destinée au dépôt et à la diffusion de documents scientifiques de niveau recherche, publiés ou non, émanant des établissements d'enseignement et de recherche français ou étrangers, des laboratoires publics ou privés.

Please use this PDF proof to check the layout of your article. If you would like any changes to be made to the layout, you can leave instructions in the online proofing interface. First, return to the online proofing interface by clicking "Edit" at the top page, then insert a Comment in the relevant location. Making your changes directly in the online proofing interface is the quickest, easiest way to correct and submit your proof.

Please note that changes made to the article in the online proofing interface will be added to the article before publication, but are not reflected in this PDF proof.

Cretaceous Research xxx (xxxx) xxx

Contents lists available at ScienceDirect

Cretaceous Research

journal homepage: www.elsevier.com/locate/CretRes

Thalassotitan atrox, a giant predatory mosasaurid (Squamata) from the upper Maastrichtian phosphates of Morocco

Nicholas R. Longrich [a, *], Nour-Eddine Jalil [b], Fatima Khaldoune [c], Oussama Khadiri Yazami [c], Xabier Pereda-Suberbiola [d], Nathalie Bardet [b]

[a] Department of Biology and Biochemistry, University of Bath, Claverton Down, Bath, BA2 7AY, United Kingdom
[b] CR2P Centre de Recherche en Paléontologie de Paris, Muséum National D'Histoire Naturelle, CP38, 57 Rue Cuvier, 75005 Paris, France
[c] Office Chérifien des Phosphates, Khouribga, Morocco
[d] Departamento de Geología, Facultad de Ciencia y Tecnología, Universidad Del Páis Vasco/Euskal Herriko Unibertsitatea, Apartado 644, 48080 Bilbao, Spain

ARTICLE INFO

Article history:
Received 18 December 2021
Received in revised form
7 July 2022
Accepted in revised form 21 July 2022
Available online xxx

Keywords:
Squamata
Mosasauridae
Mosasaurinae
Maastrichtian
K–Pg extinction
Africa

ABSTRACT

The Cretaceous–Paleogene (K–Pg) transition saw mass extinctions in terrestrial and marine ecosystems. Terrestrial vertebrate diversity patterns across the K–Pg boundary have seen extensive study, but less is known about marine vertebrates. We describe a new mosasaurid from the latest Maastrichtian phosphatic beds of Morocco, showing how mosasaurids evolved to become apex predators in the latest Cretaceous. *Thalassotitan atrox* n. gen. et sp., from the Oulad Abdoun Basin of Khouribga Province, Morocco is characterized by large size, a broad skull, massive jaws, and reduced cranial kinesis, suggesting it was highly adapted for carnivory. Teeth resemble those of killer whales in their robust, conical shape, and show heavy wear and damage. Phylogenetic analysis recovers *Thalassotitan* as a close relative of *Prognathodon currii* and *P. saturator* within the Prognathodontini. Among the associated fauna, three genera of mosasaurids, elasmosaurid plesiosaur, chelonioid turtle, and enchodontid fish show acid damage, and could be prey ingested by mosasaurids, likely *Thalassotitan*. *Thalassotitan* shows mosasaurids evolved to fill the marine apex predator niche, a niche occupied by orcas and white sharks today. Mosasaurs continued to diversify and fill new niches until their extinction at the end of the Cretaceous.
© 2022 Elsevier Ltd. All rights reserved.

1. Introduction

The Cretaceous–Paleogene (K–Pg) boundary marks a mass extinction that wiped out 90% or more of all species on Earth (Longrich et al., 2016), coinciding with the giant Chicxulub impact (Alvarez et al., 1980; Schulte et al., 2010). Although evidence increasingly favors asteroid impact as driving the extinction (Schulte et al., 2010), it has also been proposed that Late Cretaceous environmental disruptions contributed to the extinction (Archibald et al., 2010). Understanding the end-Cretaceous mass extinction requires understanding diversity up to the K–Pg boundary. While terrestrial vertebrates have seen extensive study (Archibald and Bryant, 1990; Sheehan and Fastovsky, 1992; Sheehan et al., 2000; Fastovsky and Sheehan, 2005; Longrich et al., 2011; Longrich et al., 2012; Longrich et al., 2016); less is known about marine vertebrates.

Fossils from the Late Cretaceous phosphates of Morocco (Fig. 1) have revealed a latest Maastrichtian marine vertebrate fauna, one characterized by exceptional diversity (Arambourg, 1952; Bardet et al., 2017). These fossils offer insights into the marine vertebrate turnover and ecosystem structure across the K–Pg transition (Jouve et al., 2008; Cappetta et al., 2014; Martin et al., 2017; Longrich et al., 2018). The most common reptiles in the fauna are mosasaurids (Bardet et al., 2004; Bardet et al., 2005a; Bardet et al., 2005b; Schulp et al., 2009; LeBlanc et al., 2012; Bardet et al., 2015; Longrich et al., 2021a; Longrich et al., 2021b), the dominant marine reptiles of the Late Cretaceous. Adding to the diversity of this fauna (Table 1), we describe a new, giant mosasaurid (Fig. 2) from the latest Maastrichtian of Morocco which occupied a marine apex predator niche, similar to extant orcas and white sharks.

Institutional abbreviations. MHNM – Muséum d'Histoire Naturelle de Marrakech, Marrakech, Morocco, Cadi Ayyad University; OCP – Office Chérifien des Phosphates, Khouribga, Morocco.

* Corresponding author.
E-mail address: nrl22@bath.ac.uk (N.R. Longrich).

https://doi.org/10.1016/j.cretres.2022.105315
0195-6671/© 2022 Elsevier Ltd. All rights reserved.

UNCORRECTED PROOF

Please cite this article as: N.R. Longrich, N.-E. Jalil, F. Khaldoune *et al.*, *Thalassotitan atrox*, a giant predatory mosasaurid (Squamata) from the upper Maastrichtian phosphates of Morocco, Cretaceous Research, https://doi.org/10.1016/j.cretres.2022.105315

2. Systematic palaeontology

Squamata Oppel, 1811
Mosasauridae Gervais, 1852
Mosasaurinae Gervais, 1852
Prognathodontini Russell, 1967 new definition
Prognathodontini is here defined as all species closer to *Prognathodon solvayi* than to *Globidens alabamensis* or *Mosasaurus hoffmanni*.

Thalassotitan atrox new genus and species.

Synonyms

Mosasaurus (*Leiodon*) cf. *anceps*, Arambourg, 1952
"*Mosasaurus* (*Leiodon*) cf. *anceps*", Machalski et al., 2003
Prognathodon sp., Bardet et al., 2004
Prognathodon sp. nov., Bardet et al., 2008
Prognathodon sp. nov., Bardet et al., 2010
Prognathodon sp. nov., Bardet, 2012
Prognathodon sp., Cappetta et al., 2014
Prognathodon sp. nov., Bardet et al., 2015
Prognathodon sp. nov., Bardet al., 2017
Prognathodon aff. *saturator*, Longrich et al., 2021a
Prognathodon aff. *saturator*, Longrich et al., 2021b

Etymology. Greek *thalassa*, 'sea', and *titan*, 'giant'; *atrox*, 'cruel, merciless'.

Diagnosis. Large mosasaurid, ~1.5 m skull length and ~9–10 m total length (Fig. 2). Premaxilla tip short and blunt. Interlocking contacts between premaxilla and maxilla. Maxilla deep, ventral margin convex. Interdigitating joint between maxilla and prefrontal formed by a series of tongue-and-groove joints, with margins of the joint interdigitating. Prefrontal broadly overlaps onto frontal. Prefrontal-postorbitofrontal excluding frontal from orbital margin. Frontal short, broad, strongly constricted anteriorly and strongly concave at contact with parietal anterolateral wings; postorbital processes displaced anteriorly; large posteromedial processes wrapping around parietal foramen. Jugal broad and robust where

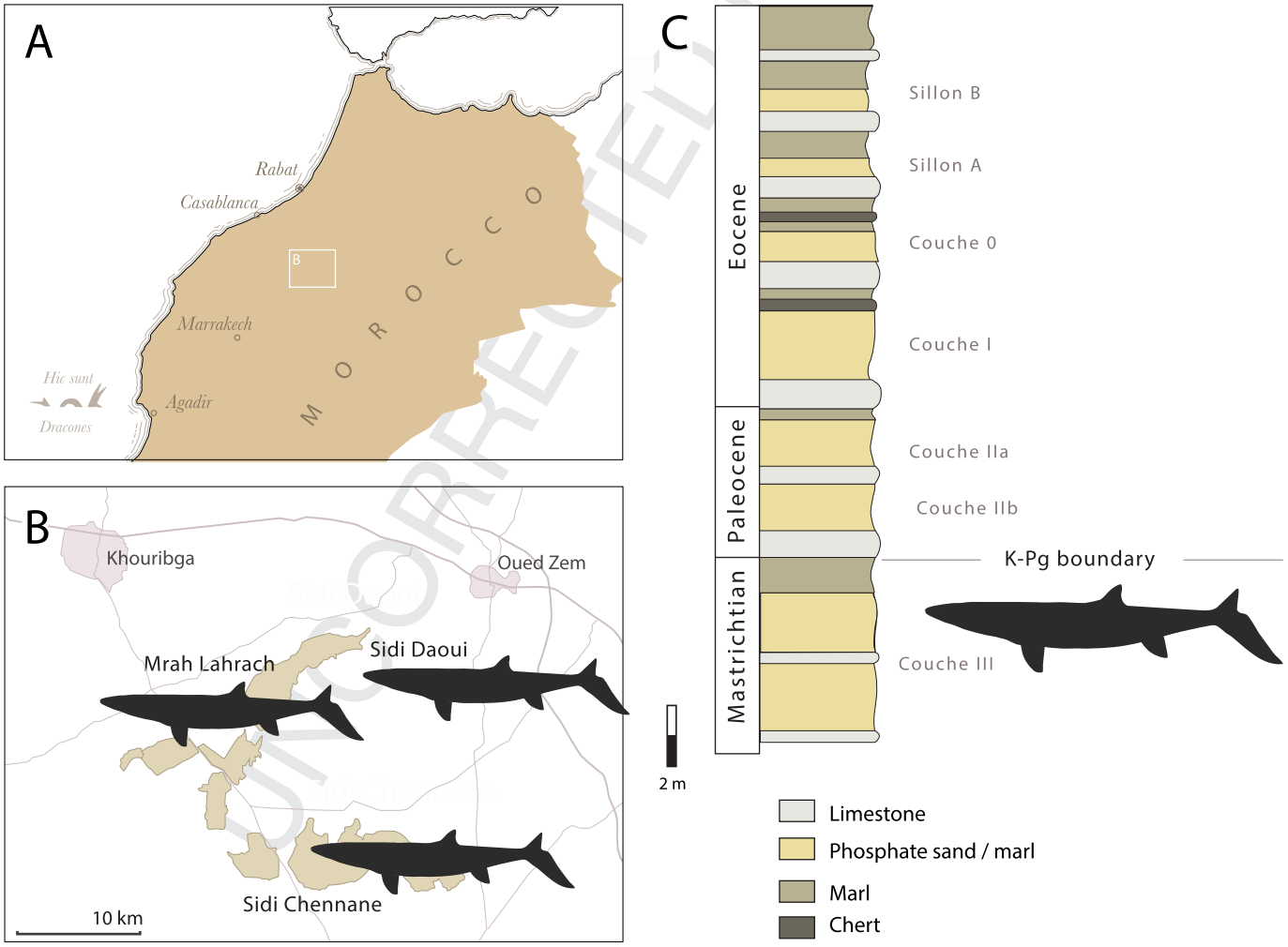

Fig. 1. A, map of northern Morocco showing the location of the new mosasaurid; B, map of the Oulad Abdoun Basin of Khouribga Province, showing the Sidi Daoui, Mrah Lahrach and Sidi Chennane phosphate mines; C, synthetic stratigraphic column of the Oulad Abdoun phosphatic series showing the position of the new mosasaurid.

UNCORRECTED PROOF

Table 1
Marine squamates from Upper Couche III phosphates, late Maastrichtian, Oulad Abdoun Basin, Khouribga Province, Morocco.

Mosasauridae	
Mosasaurinae	
Thalassotitan atrox n.gen. et sp.	This paper
Mosasaurus beaugei	Arambourg (1952)
Prognathodon currii	Christiansen and Bonde (2002)
Globidens phosphaticus	Bardet et Pereda-Suberbiola (2005b)
Eremiasaurus heterodontus	LeBlanc et al. (2012)
Carinodens minalmamar	Schulp et al. (2009)
Xenodens calminechari	Longrich et al. (2021a)
Halisaurinae	
Halisaurus arambourgi	Bardet and Pereda-Suberbiola (2005a)
Pluridens serpentis	Longrich et al. (2021b)
Plioplatecarpinae	
Gavialimimus almaghribensis	Strong et al. (2020)
Pachyvaranidae	
Pachyvaranus crassispondylus	Arambourg (1952)

its contacts the maxilla. Quadrate massive with large, fused supra- and infrastapedial processes below median part of the shaft. Mandible robust. Dentary wide and short, bowed. Tall, triangular coronoid process. Two premaxillary, twelve maxillary and fourteen dentary teeth. Marginal teeth massive, conical, and weakly curved. Pterygoid teeth large, about the same size and shape than the marginal ones. Tooth crowns with anastomosed ornamentation of apex and serrated anterior and posterior carinae. Humerus short and robust. Radius with large anterior process giving it a sub-rectangular to crescent-like shape.

Thalassotitan atrox can be distinguished from *Prognathodon solvayi* Dollo (1889) in its overall larger size, higher tooth count, robust tooth crowns lacking longitudinal ridges, weakly prognathous dentition, shorter frontal, more elongate parietal and more robust jugal. It differs from *Prognathodon saturator* Dortangs et al. (2002) in having more robust tooth crowns, lack of prefrontal overlap onto frontals, a shortened frontal, frontals with anterolateral processes that hook around the nares and with anteriorly displaced postorbital processes, smaller parietal foramen, more robust jugal, and more strongly expanded stapedial process of the quadrate. It differs from *Prognathodon currii* Christiansen and Bonde (2002) in having teeth with pointed apices and weakly developed ornamentation, a shallower maxilla premaxillary process, and a more gracile, weakly curved dentary. Differs from *Prognathodon lutigini* Yakovlev (1901) in the higher tooth count and larger size. Differs from *Prognathodon giganteus* Dollo (1904) in having a steeper maxilla–premaxilla contact, a more robust jugal, a more massive mandible, and more robust tooth crowns. Differs from *Prognathodon overtoni* Williston (1897) in being larger with a shorter rostrum, a shorter, anteriorly narrow frontal with an anteriorly displaced postorbital processes, a longer parietal, more robust jugal, deeper mandible, and taller coronoid process.

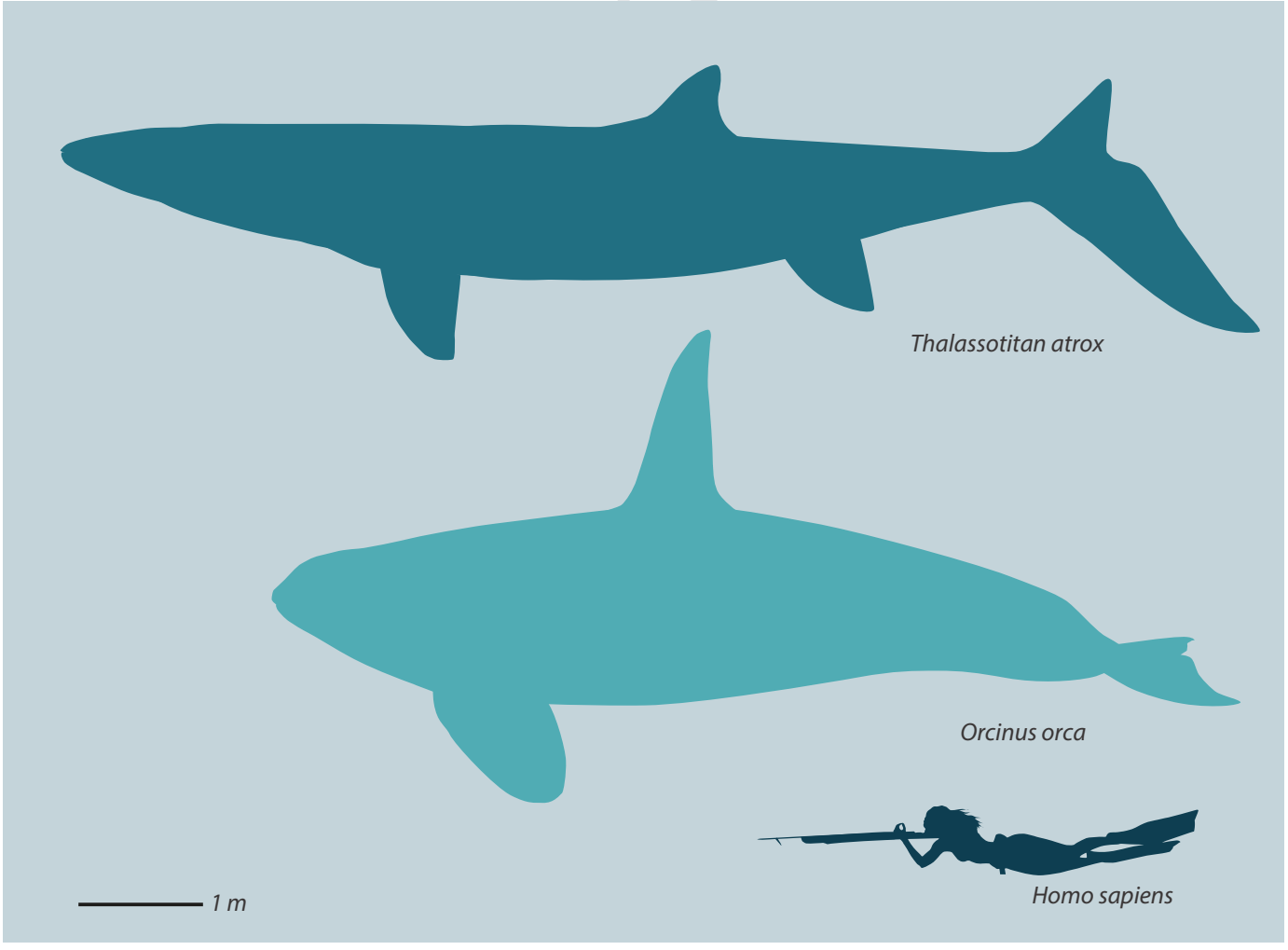

Fig. 2. Relative size of *Thalassotitan atrox*, *Orcinus orca*, and *Homo sapiens*.

Syntypes. MNHM.KH.231, skull, mandible, cervical and dorsal vertebrae, ribs (Figs. 3–5); OCP DEK-GE 417, skull and mandible, cervical and dorsal vertebrae, ribs, pectoral girdle and forelimb (Fig. 6).

Referred Material. OCP DEK-GE 109, mandible and incomplete skull, cervical and dorsal vertebrae, ribs (Fig. 7); OCP DEK-GE 10, maxillae, dentaries, and dorsal vertebrae (Fig. 8); OCP DEK-GE 497, skull and incomplete mandible, associated limb bones (Fig. 9); MNHM.KH.324, skull and jaws (Fig. 10); MNHM.KH.1047, frontal, right maxilla and rib (Fig. 11); MNHM.KH.326, dentary and maxilla (Fig. 12); MNHM.KH.396, right maxilla (Fig. 13); MNHM.KH.325, right dentary (Fig. 14); MHNM.KH.330, left dentary (Fig. 15A) MHNM.KH.1253, right dentary (Fig. 15B); MHNM.KH.1051, dorsal vertebrae and ribs (Fig. 16); OCP DEK-GE 90, incomplete skull and mandible (not figured), cervical vertebrae; OCP DEK-GE 98, incomplete jaws (not figured).

A number of isolated teeth from Africa, the Middle East, and Brazil may belong to *Thalassotitan atrox* or closely related species. From the phosphatic basins of Morocco, Arambourg (1952) described under the name of *Mosasaurus* (*Leiodon*) cf. *anceps* a number of different teeth, some of which appear to represent *T. atrox*. The discovery of skulls with teeth *in situ*, allow referral of the smaller and more slender ones to *Eremiasaurus heterodontus* LeBlanc et al., 2012; the larger and more robust ones almost certainly belong to *Thalassotitan atrox* (see discussion in Bardet, 2012 and LeBlanc et al., 2012).

Similar teeth also occur in the Maastrichtian of the Ganntour Basin in Morocco (Cappetta et al., 2014, Fig 8O,P), Poland (Machalski et al., 2003: Fig. 8), Jordan (Bardet and Pereda-Suberbiola, 2002: Fig. 2G); Israel (NB pers. obs. based on Raab, 1963), Egypt (NB pers. obs. based on Gemmellaro, 1921), Angola (Schulp et al., 2013a: Fig1a-c), and Brazil (NB pers.obs. based on Price, 1957) (see Bardet, 2012 for a complete discussion). These may represent *T. atrox* or an allied taxon, such as *P. saturator*.

Locality, Horizon, and Age. Thalassotitan comes from the phosphates of the Oulad Abdoun Basin, Khouribga Province, Morocco (Fig. 1). The basin's exposed deposits form a wide "C" shape. The northern part is named Sidi Daoui, the central one is known as Mrah Lahrach and the southern one is called Sidi Chennane. Some specimens come from excavations made in the framework of the French–Morocco PhosphaPal Program of scientific collaboration; while others were excavated by local fossil collectors; in this last case, information on provenance is based on discussions with collectors as well as the lithology of the phosphatic series.

Syntypes and most referred specimens come from Sidi Daoui, where the species is among the most common mosasaurids in terms of skeletal remains and shed teeth. One specimen (OCP DEK-GE 109) was unearthed in Mrah Lahrach, and a referred dentary (MNHM.KH.330) comes from coeval beds at Sidi Chennane ~20 km away. Shed teeth of *Thalassotitan* are also highly abundant at both Daoui Sidi Chennane (NRL, pers. obs.).

The phosphates were deposited in a shallow embayment of the eastern Atlantic, which flooded North Africa in the Late Cretaceous and Early Paleogene (Bardet et al., 2017). Within the phosphates of the Oulad Abdoun Basin, *Thalassotitan* occurs in Upper Couche III (Fig. 1C), which is correlated with the latest Maastrichtian by biostratigraphy (Cappetta, 1987) and chemostratigraphy (Kocsis et al., 2014). This level was deposited ~1 Ma or less before the K–Pg boundary.

Upper Couche III consists of phosphatic sands derived from bone, teeth, scales, and coprolites. The layer hosts laterally extensive (tens of kilometers) bonebeds. In addition to at least ten mosasaurid species (see Table 1), these beds are rich in sharks (Arambourg, 1952), fish (Arambourg, 1952), plesiosaurs (Vincent et al., 2011), sea turtles (Bardet et al., 2013; Lapparent de Broin et al., 2013), crocodylomorphs (Jouve et al., 2008), and pterosaurs (Pereda-Suberbiola et al., 2003; Longrich et al., 2018). Dinosaurs are present, but rare (Pereda-Suberbiola et al., 2004; Longrich et al., 2017; Longrich et al., 2021c).

Description (Figs. 3–16). The syntypes permit a complete description of the skull, mandible, dentition, and the anterior postcranial skeleton, including cervical and dorsal vertebrae, pectoral girdle and forelimb. Referred specimens provide additional information. Overall, the skull and skeleton resemble *Prognathodon saturator* (Dortangs et al., 2002) and *P. currii* (Christiansen and Bonde, 2002), and to a lesser degree, the smaller, more primitive *P. solvayi* (Lingham-Soliar and Nolf, 1989) and *P. overtoni*.

Skull

Premaxilla. The premaxilla bears four teeth, as typical of Mosasauridae (Russell, 1967). In some specimens (OCP DEK-GE 10, 98, 497) premaxillary teeth appear procumbent, but this may be preservational, as this feature is absent in others. The premaxilla's body is low, remarkably short, broad and widely convex in dorsal view, similar to *Varanus*. It is small relative to the skull, as in *P. currii* (Christiansen and Bonde, 2002) and *P. solvayi* (Lingham-Soliar and Nolf, 1989). A large predental prominence is retained in *P overtoni* (Konishi et al., 2011) but absent in *T. atrox*, as in *P. solvayi* (Lingham-Soliar and Nolf, 1989) and *P. currii* (Christiansen and Bonde, 2002). The premaxilla's body bears multiple large neurovascular foramina, as in other mosasaurids (Russell, 1967), likely associated with tactile nerves (Álvarez-Herrera et al., 2020; Longrich et al., 2021a). Foramina radiate out from the premaxilla's tip and extend onto the dorsal surface. The premaxilla's narial process is broad between the maxillae, as in *P. currii* (Christiansen and Bonde, 2002) but not *P. solvayi* (Lingham-Soliar and Nolf, 1989). It extends back between the nares as a broad, tongue-shaped extension with parallel margins, then tapers between the external nares to form a slender rod that contacts the frontals. Between the maxillae, the premaxilla's dorsal surface has a keel. The keel is well marked, being either smooth or with a sharp dorsal edge, but is low and short relative to Mosasaurini such as *Mosasaurus hoffmanni* (Lingham-Soliar, 1995; Street and Caldwell, 2017). *P. solvayi* lacks a keel (Lingham-Soliar and Nolf, 1989).

The premaxilla–maxilla contact forms a complex, interdigitating suture. Unusually, the premaxilla bears flanges and grooves that interdigitate with the maxillae, restricting movement between them. This interlocking contact is a specialization of *Thalassotitan* or perhaps Prognathodontini, being absent from e.g. *Mosasaurus* (Street and Caldwell, 2017). A similar interlocking contact occurs in the nasal-maxilla joint of the tyrannosaurid dinosaurs *Tyrannosaurus rex* and *Tarbosaurus baatar* (Snively et al., 2006).

Maxilla. The maxilla has 12 alveoli, as in *P. saturator* (Dortangs et al., 2002) and *P. solvayi* (Lingham-Soliar and Nolf, 1989). *P. overtoni* has 12–13 maxillary teeth; *P. currii* has 11 (Christiansen and Bonde, 2002). The maxilla is short, robust and deep as in *P. solvayi* and *P. currii*. The maxilla of *P. saturator* is damaged and cannot be compared (Dortangs et al., 2002).

The premaxillary suture is tall in lateral view and broadly rounded as in *P. overtoni*. Its anterodorsal margin forms a 60° angle where it contacts the body of the premaxilla, as in *P. currii*. Farther back the suture forms shallower angle, about 30°. The premaxilla–maxilla suture ends between the third and fourth teeth, as in *P. solvayi* (Lingham-Soliar and Nolf, 1989) and *P. overtoni* (Konishi et al., 2011). As in other Prognathodontini (Lingham-Soliar and Nolf, 1989), the maxilla's concave dorsal edge forms the nares' lateral margin. Posteriorly, a tall, sharp triangular ascending process contacts the prefrontals in a straight, oblique suture, followed by a small

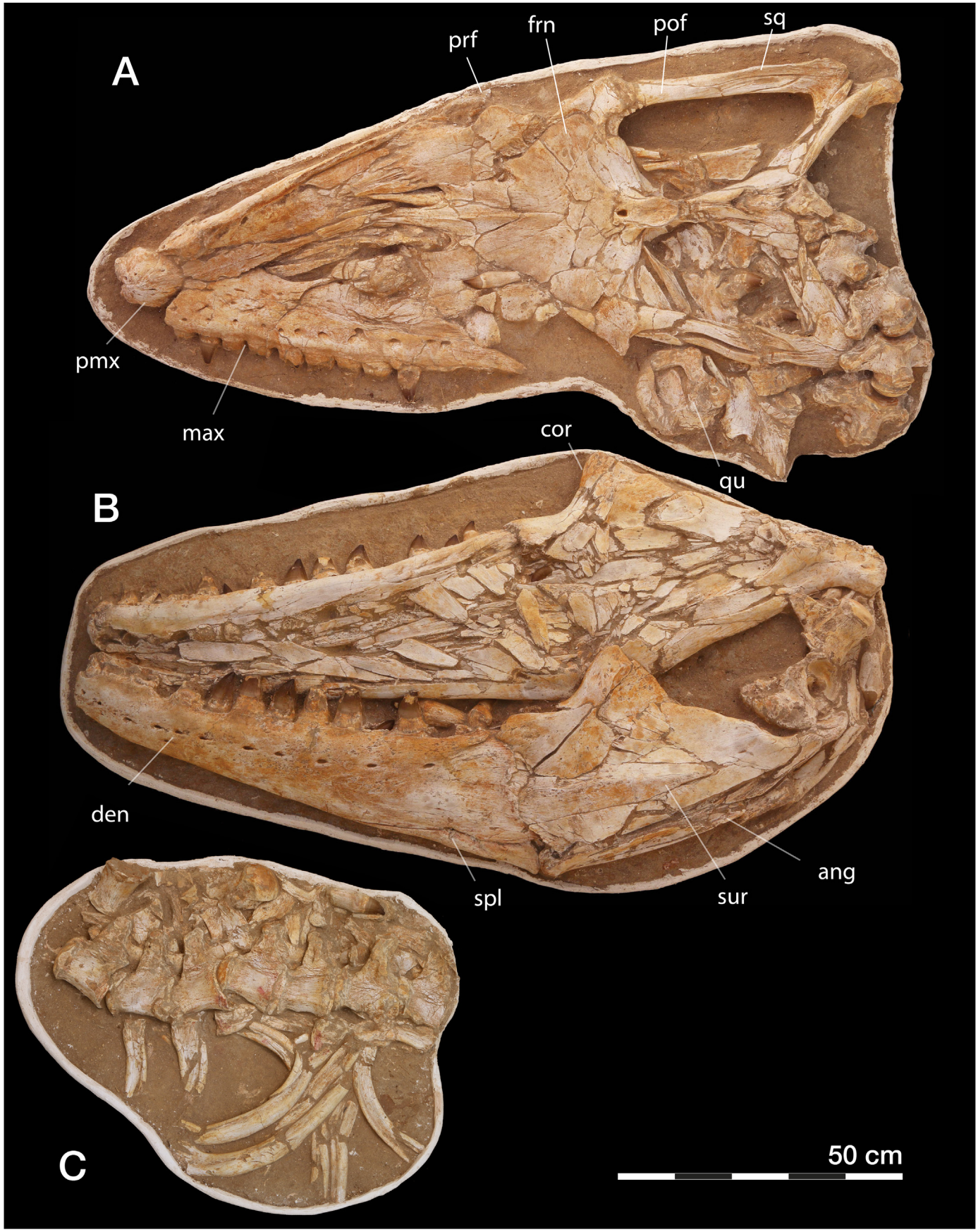

Fig. 3. *Thalassotitan atrox,* syntype MNHM.KH.231, skull, mandible and articulated dorsal vertebrae and ribs, late Maastrichtian age, Upper Couche III of Sidi Daoui, Oulad Abdoun Basin, Morocco. Abbreviations: ang, angular; cor, coronoid process; den, dentary; frn, frontal; max, maxilla; pmx, premaxilla; pof, postfrontal; prf, prefrontal; qu, quadrate; spl, splenial; sq, squamosal; sur, surangular.

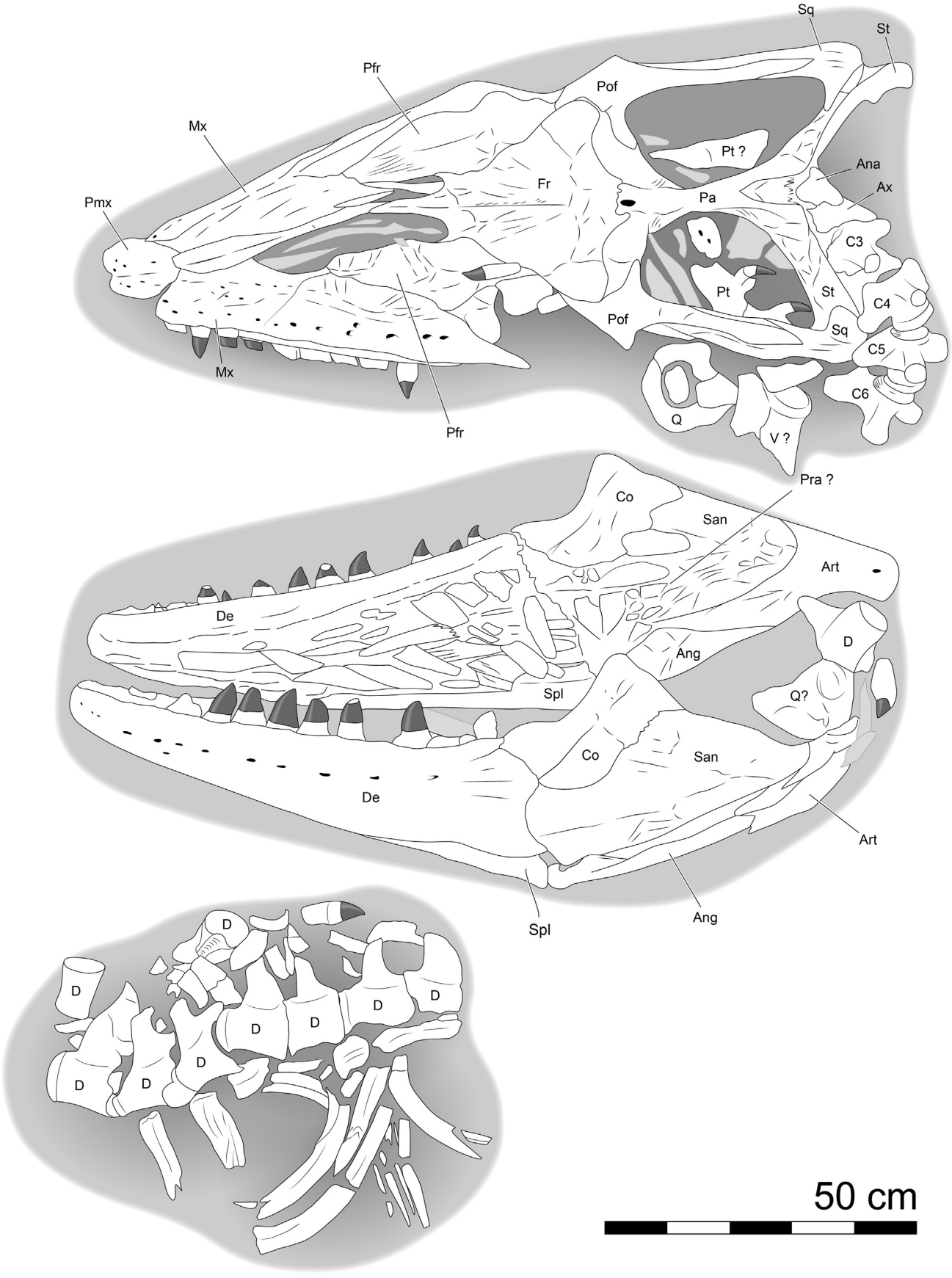

Fig. 4. *Thalassotitan atrox,* syntype MNHM.KH.231, skull, mandible and articulated dorsal vertebrae and ribs, late Maastrichtian age, Upper Couche III of Sidi Daoui, Oulad Abdoun Basin, Morocco, interpretive drawing. Abbreviations: Ana, atlantal neural arch; Ang, angular; Art, articular; Ax, axis; C1–C6, cervicals 1–6; Co, coronoid, D, dorsal vertebrae; De, Dentary; Fr, frontal; Mx, maxilla; Pfr, prefrontal; Pmx, premaxilla, PoF, postorbitofrontal; Pt, pterygoid; Q, quadrate; San, surangular; Spl, splenial; St, supratemporal; V, vomer.

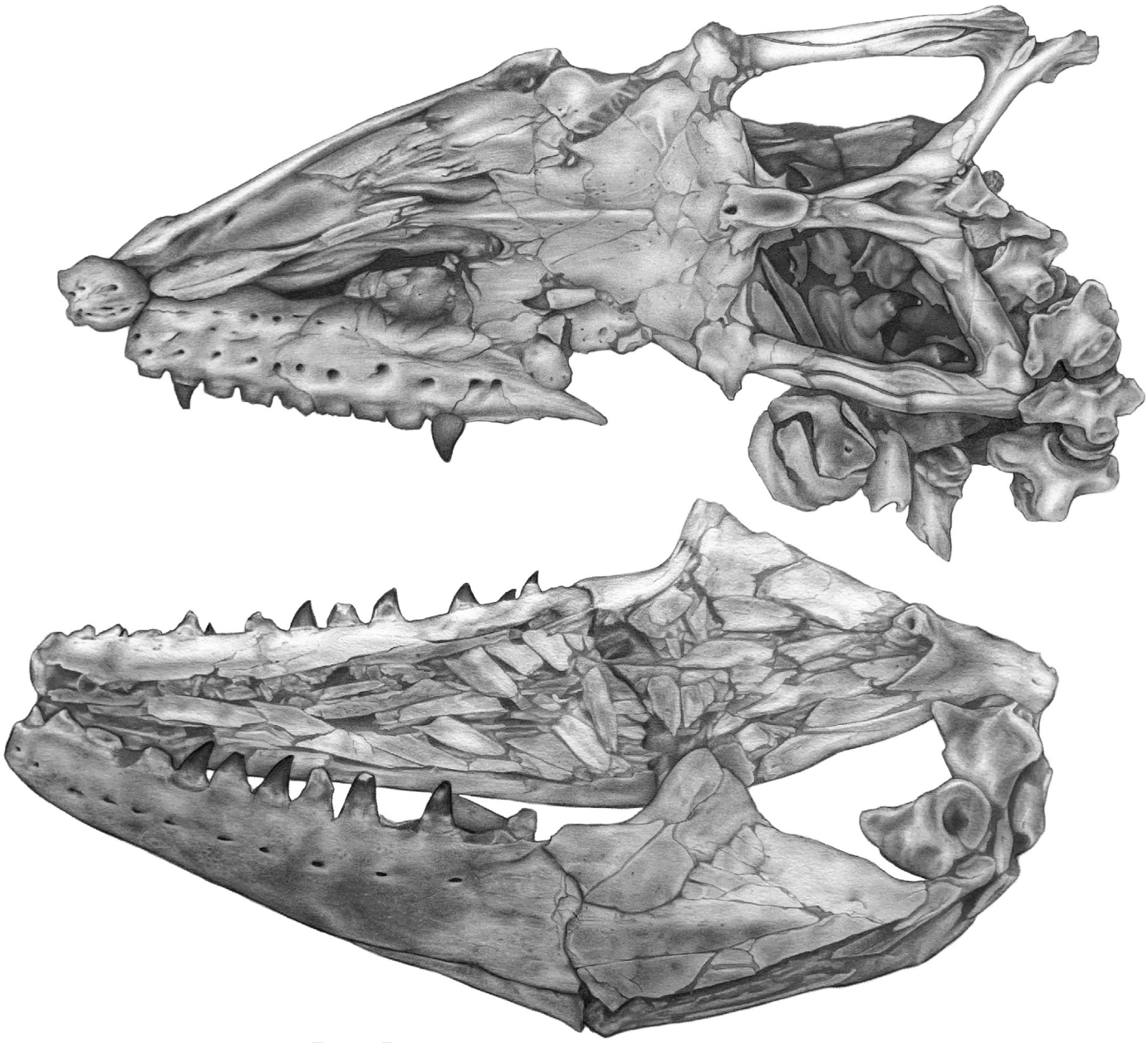

Fig. 5. *Thalassotitan atrox,* syntype MNHM.KH.231, skull and mandibles. Art by Magdalena Cygan.

posterolateral process. The maxilla then tapers posteriorly in a sharp extremity. It has a broad suture for the jugal, with ridges and grooves where the two bones overlapped. The maxilla's ventral margin is straight but can be slightly convex in large specimens. A similar condition is seen in *P. saturator* (Schulp, 2006).

The maxilla's lateral surface is flat except for a low, broad ridge above the toothrow. Large neurovascular foramina pierce the maxilla's tip, and extend posteriorly in a row running along the bone's ventral margin, becoming larger posteriorly. The bone's surface is sculptured and rugose, especially in large individuals, with large, anastomosing grooves for blood vessels.

Jugal. The jugal resembles that of *P. currii* (Christiansen and Bonde, 2002) and *P. saturator* (Dortangs et al., 2002), in being L-shaped, with a short, broad ascending ramus and a longer suborbital ramus, which is weakly curved. The two rami form a right angle, giving the bone an "L" shape. The suborbital ramus is massive. Anteriorly it forms a broad tongue where it overlaps the maxilla, posteriorly it is dorsoventrally narrow, but transversely broad. In *P. overtoni* (Konishi et al., 2011) and *P. solvayi* (Lingham-Soliar and Nolf, 1989) the suborbital ramus is slender, bowed, and lacks an anterior expansion. The posterior process is reduced. The ascending ramus is short and broad and slightly tapers where it meets the postorbitofrontal.

Nasal. In MHNM.KH.231 and OCP DEK-GE 497 large, well-developed nasals are present. They are long, slender rod-like bones bordering the premaxillary internarial bar posterolaterally. They form the posteromedial margin of the nares. Anteriorly, the nasals taper to merge with the premaxillary internarial bar. Posteriorly, they abut against the frontal medially in a convex suture. Nasals are highly reduced in mosasaurids (Russell, 1967; Gauthier et al., 2012) and rarely preserved, but are seen in some mosasaurids, including *Eonatator coellensis* (Páramo-Fonseca, 2013),

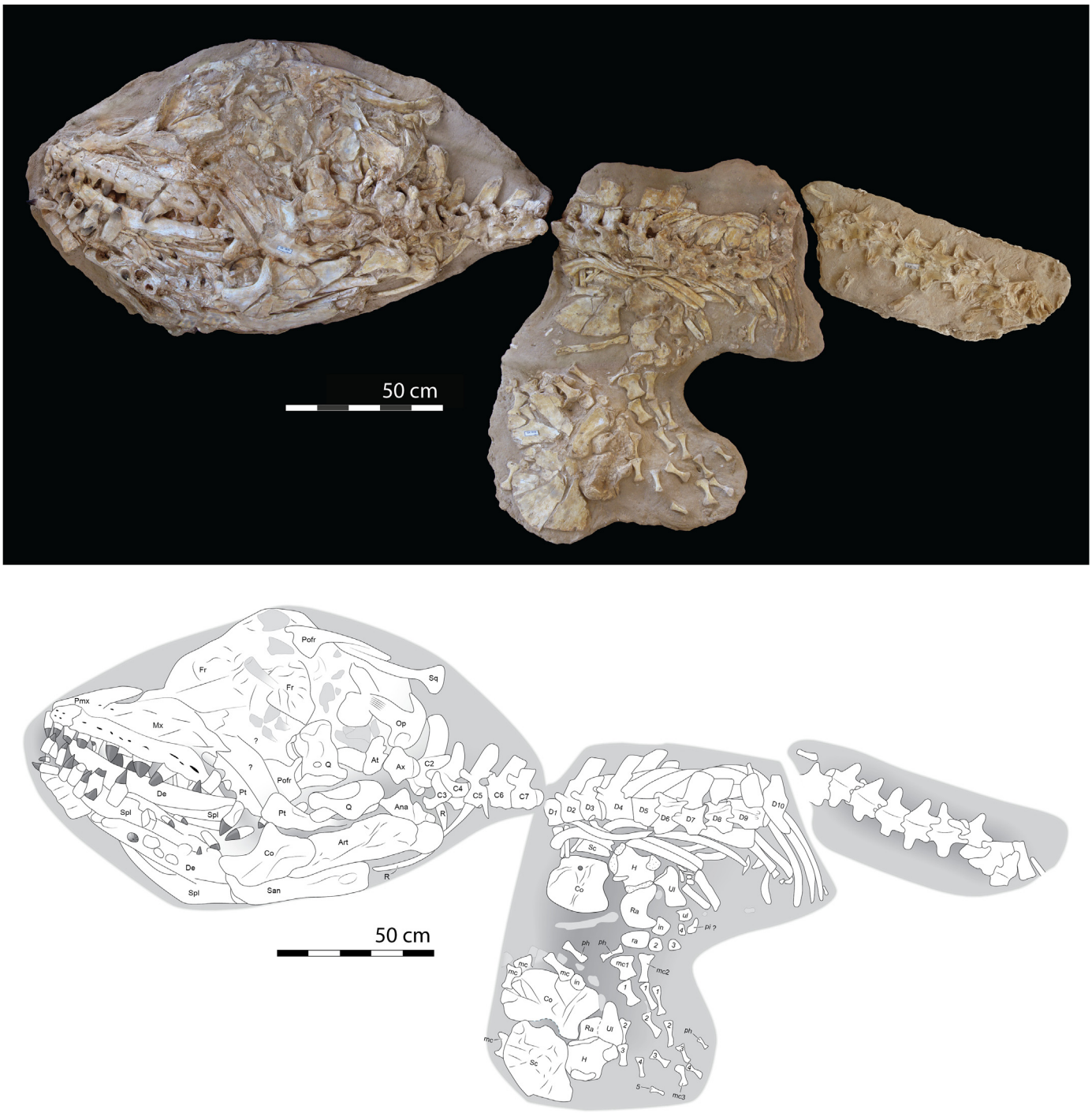

Fig. 6. *Thalassotitan atrox,* syntype OCP DEK-GE 417, skull, mandible, articulated cervical, dorsal vertebrae and ribs, pectoral girdle and forelimb, late Maastrichtian age, Upper Couche III of Sidi Daoui, Oulad Abdoun Basin, Morocco, photograph and interpretive drawing. Abbreviations: Art, articular; At, atlas; Ax, axis; Co, coronoid; C2–C7, cervicals 2–7; De, dentary; Fr, frontal; Mx, maxilla; Op, opisthotic; Pofr, Postorbitofrontal; Pmx, premaxilla; Pt, pterygoid; Q, quadrate; San, surangular; Spl, splenial; Sq, squamosal.

Pluridens serpentis (Longrich et al., 2021a), *Plotosaurus bennisoni*, *Eonatator sternbergi*, and *Tylosaurus* (Russell, 1967).

External naris. The nares extend from the 4th to the 10th maxillary tooth position. The nares are bordered by premaxillae, maxillae, prefrontals and nasals. In lateral and dorsal views the narial embayment of the maxilla is complex. It is sigmoid in shape, being divided into two parts by a bulge located at the 6–7th tooth positions. A short, deep concavity lies anteriorly between tooth position 4 and 6, and a longer, less concave one posteriorly.

Lacrimal. This bone is only observable isolated, in OCP DEK-GE 109. It has the "L" shape typical of mosasaurids (Russell, 1967).

Prefrontal. The prefrontal is a large, triangular bone contacting the maxillae anteriorly, and the frontals and postorbitofrontals posteriorly. It forms the posterolateral margins of the nares, and the anterodorsal margins of the orbits.

The maxillary suture broadly underlaps the posterodorsal wing of the maxilla. This contact bears long, parallel grooves and flanges, forming a series of tongue-and-groove joints with the maxilla. The

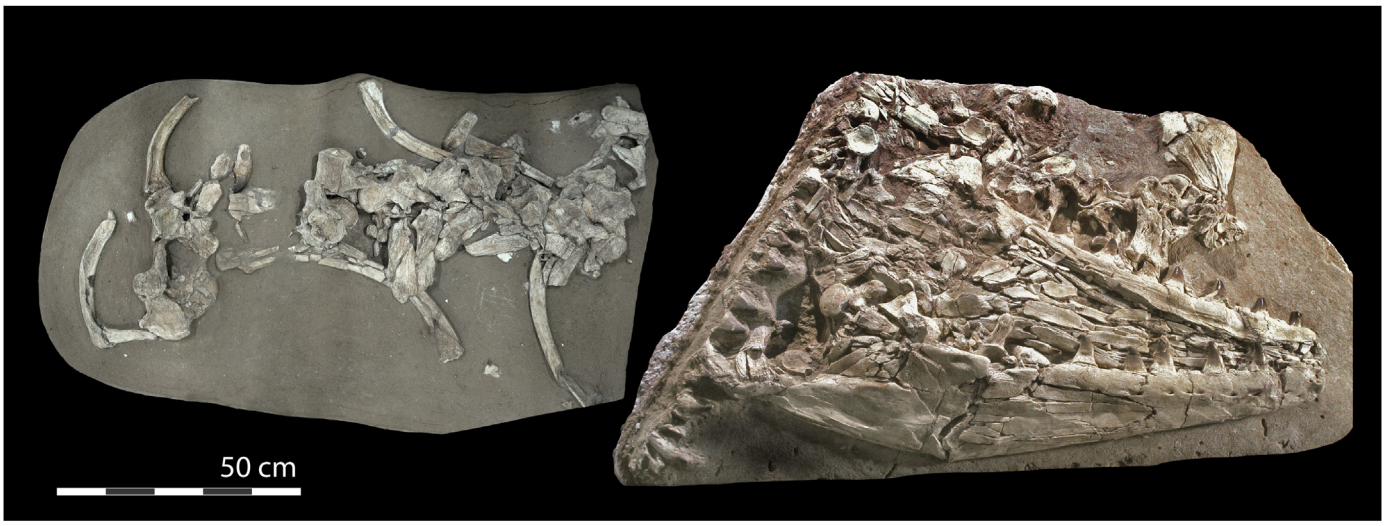

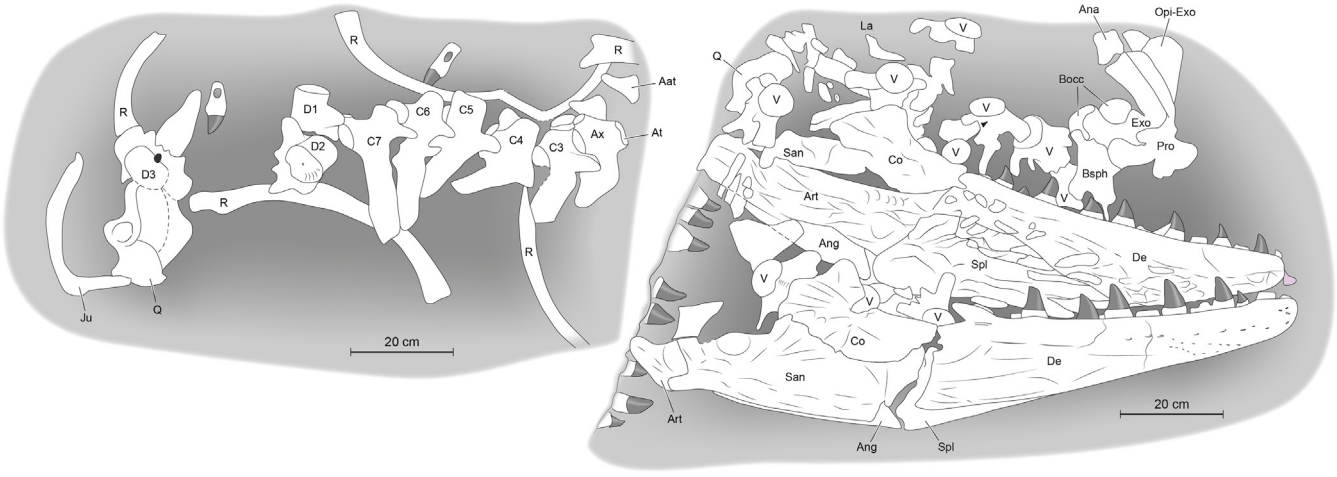

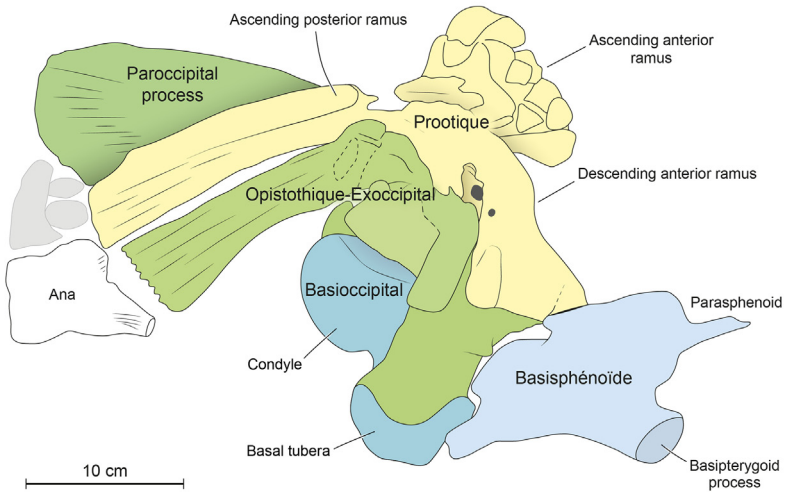

Fig. 7. *Thalassotitan atrox,* A, referred specimen OCP DEK-GE 109, mandible, incomplete skull, cervical and dorsal vertebrae, ribs, late Maastrichtian age, Upper Couche III of Mrah Lahrach, Oulad Abdoun Basin, Morocco. Abbreviations: Ana, atlantal neural arch; Ang, angular; Art, articular; Ax, axis; Bsph, Basisphenoid; C3–C7, cervical 3–7; Co, coronoid; De, dentary; D1–D2, dorsal 1 and 2; Exo, exoccipital; La, lacrimal; Opi-Exo, opisthotic-exoccipital; Pro, prootic; Q, quadrate; R, rib; San, surangular; Spl, Splenial; V, vertebrae.

Fig. 8. *Thalassotitan atrox*, referred specimen OCP DEK-GE 10, mandible, incomplete skull, cervical vertebrae, late Maastrichtian age, Upper Couche III of Sidi Daoui, Oulad Abdoun Basin, Morocco. B, referred specimen OCP DEK-GE 109, mandible, incomplete skull, cervical and dorsal vertebrae, ribs, late Maastrichtian age Upper Couche III of Mrah Lahrach, Oulad Abdoun Basin, Morocco.

joint's margin is interdigitating, with small finger-like processes of the maxilla's posterodorsal wing projecting posteriorly to interlock with the prefrontal.

The prefrontal's dorsal surface bears a small tab overlapping the frontals behind the nares, pinching the frontals in dorsal view. This overlap may occur in *P. currii*, but seems to be absent in *P. saturator* and other Prognathodontini (Schulp, 2006).

As in other mosasaurids, there is a supraorbital ridge. This ridge forms a laterally projecting shelf, a derived feature of Mosasaurinae. The shelf is shaped like a blunt triangle, similar to *P. currii* (Christiansen and Bonde, 2002), but smaller than that of *P. solvayi* (Lingham-Soliar and Nolf, 1989) and *P. overtoni* (Konishi et al., 2011). Posteriorly, the prefrontal has a broad flange underlapping the frontals. Its dorsal surface bears a series of low ridges separated by broad grooves, creating another set of interlocking joints. The prefrontal's posterior tip contacts the postorbitofrontal, excluding the frontals from the margin of the orbit, as in other Prognathodontini (Konishi et al., 2011) and Mosasaurini (Lingham-Soliar, 1995).

Frontal. As in other mosasaurids (Russell, 1967), the fused frontals contact the premaxillae and nasals anteriorly, the prefrontals anterolaterally, the postorbitofrontals posterolaterally, and the parietals posteriorly.

The frontal is short and broad, and shaped almost like an isosceles triangle, with straight, anteriorly converging lateral margins. It resembles that of *P. currii*. The frontal in *P. saturator* and *P. solvayi* is more elongate, and wider anteriorly (Schulp, 2006).

The frontal's dorsal surface bears a median ridge, as in other Mosasauridae, extending to the center of the frontal. The ridge is low, but with a sharp edge. The ridge's morphology resembles that of *P. overtoni* (Konishi et al., 2011). The frontal ridge is lost in *P. solvayi* (Lingham-Soliar and Nolf, 1989) and this area is damaged in *P. currii* and *P. saturator*, preventing comparison. Large neurovascular foramina lie in the center of the frontals. Similar foramina occur in other Mosasaurinae, Plioplatecarpinae, and Tylosaurinae, but are absent from Halisaurinae (Polcyn et al., 2012) and *Tethysaurus nopcsai* (Bardet et al., 2003).

The frontal premaxillary process is long and narrow. Anteriorly it splits where it contacts the premaxillae. Laterally, the narial processes hook anteriorly, forming the nares' caudal and caudolateral margins. Similar hooked narial processes occur in *P. currii* (Christiansen and Bonde, 2002) and *P. saturator*, but not *P. solvayi* (Konishi et al., 2011) or *P. overtoni* (Konishi et al., 2011).

Posterior to the narial process, the frontal's lateral margin is sigmoidal in dorsal view. The frontal is constricted between the prefrontals, behind the nares; next the lateral margins become strongly convex, overlapping onto the prefrontals. Then the frontal is slightly constricted between the orbits. Finally the frontal forms a broadly convex postorbital process where it contacts the end of the prefrontal and the postorbitofrontal. The frontals are excluded from the orbital margin by the prefrontal-postorbitofrontal contact.

The postorbitofrontal processes have a broad and rounded anterior margin, as in most Mosasaurinae (Lingham-Soliar, 1995; Schulp, 2006) other than *Clidastes* (Lively, 2018). The postorbitofrontal processes are displaced anteriorly relative to the midline fronto-parietal contact, unlike *P. saturator*, *P. solvayi*, and *P. overtoni* (Schulp, 2006). Medial to these corners, the frontal-parietal contact is strongly concave. A similar concave margin occurs in *P. saturator* (Schulp, 2006), *P. currii* (Christiansen and Bonde, 2002) and *P. overtoni* (Konishi et al., 2011), but is less well-developed. A disarticulated specimen shows that a crescentic lappet of the parietals broadly overlapped the frontals here, reducing flexibility across the fronto-parietal joint.

Medial to this concavity the posteromedial flanges of the frontal wrap around the parietal table, as in *P. saturator* (Schulp, 2006), *P. currii* (Christiansen and Bonde, 2002), and *Mosasaurus* spp. (Lingham-Soliar, 1995; Konishi et al., 2014). The median contact between the frontals and the parietal table is narrow, about 15% of the width across the postorbital processes. A similar condition occurs in *P. saturator* (Schulp, 2006), *Mosasaurus* and *Tylosaurus* (Bell, 1997). The frontal is excluded from the parietal foramen, as in *P. saturator* and *P. overtoni*, but in contrast to *P. solvayi* (Schulp, 2006).

UNCORRECTED

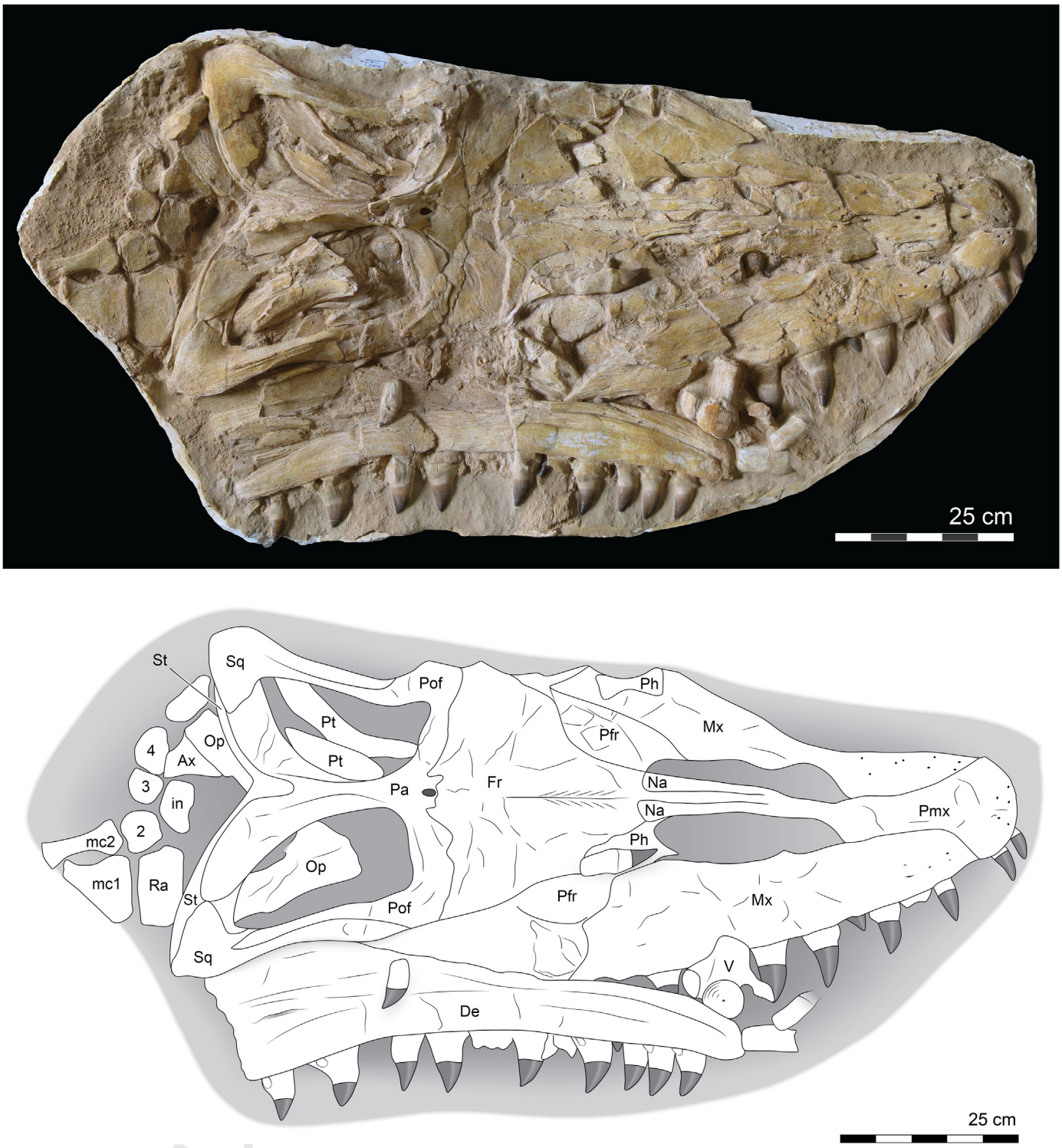

Fig. 9. *Thalassotitan atrox,* referred specimen OCP DEK-GE 497, skull, mandible, disarticulated forelimb elements, late Maastrichtian age, Upper Couche III of Sidi Daoui, Oulad Abdoun Basin, Morocco. Teeth are restored. Abbreviations: Ax, axis; De, dentary; in, intermedium; Mc1, metacarpal I; Mc2, metacarpal 2; Mx, maxilla; Na, nasal; Op, opisthotic; Ph, phalanx; Pfr, prefrontal; Pof, postorbitofrontal; Pmx, premaxilla; Pt, pterygoid; Ra, radiale; Sq, squamosal; St, supratemporal; 2,3,4 = distal carpals 2, 3, 4.

As a result, the fronto–parietal suture has a complex shape, with the parietal extending anteriorly onto the lateral wings of the frontal and the frontal extending posteriorly around the parietal table. This created an interlocking articulation, greatly limiting movement across the fronto-parietal suture, especially when biting down. Lingham-Soliar (1995) and LeBlanc et al. (2013) have discussed the flexibility of the mesokinetic joint in the mosasaurid skull using the frontal-parietal suture shape as a proxy. Large taxa such as *Tylosaurus* (Bell, 1997) and derived Mosasaurini like *Mosasaurus*, *Prognathodon* and *Plotosaurus* (Lingham-Soliar, 1995; Schulp, 2006; LeBlanc et al., 2013) lose the mesokinetic joint, independent of their diet. This results from a large extension of the

Fig. 10. *Thalassotitan atrox*, referred specimen MHNM.KH.324, late Maastrichtian age, Upper Couche III of Sidi Daoui, Oulad Abdoun Basin, Morocco. A, skull and mandible; B, closeup of the teeth, showing toothwear and pathologies (arrows).

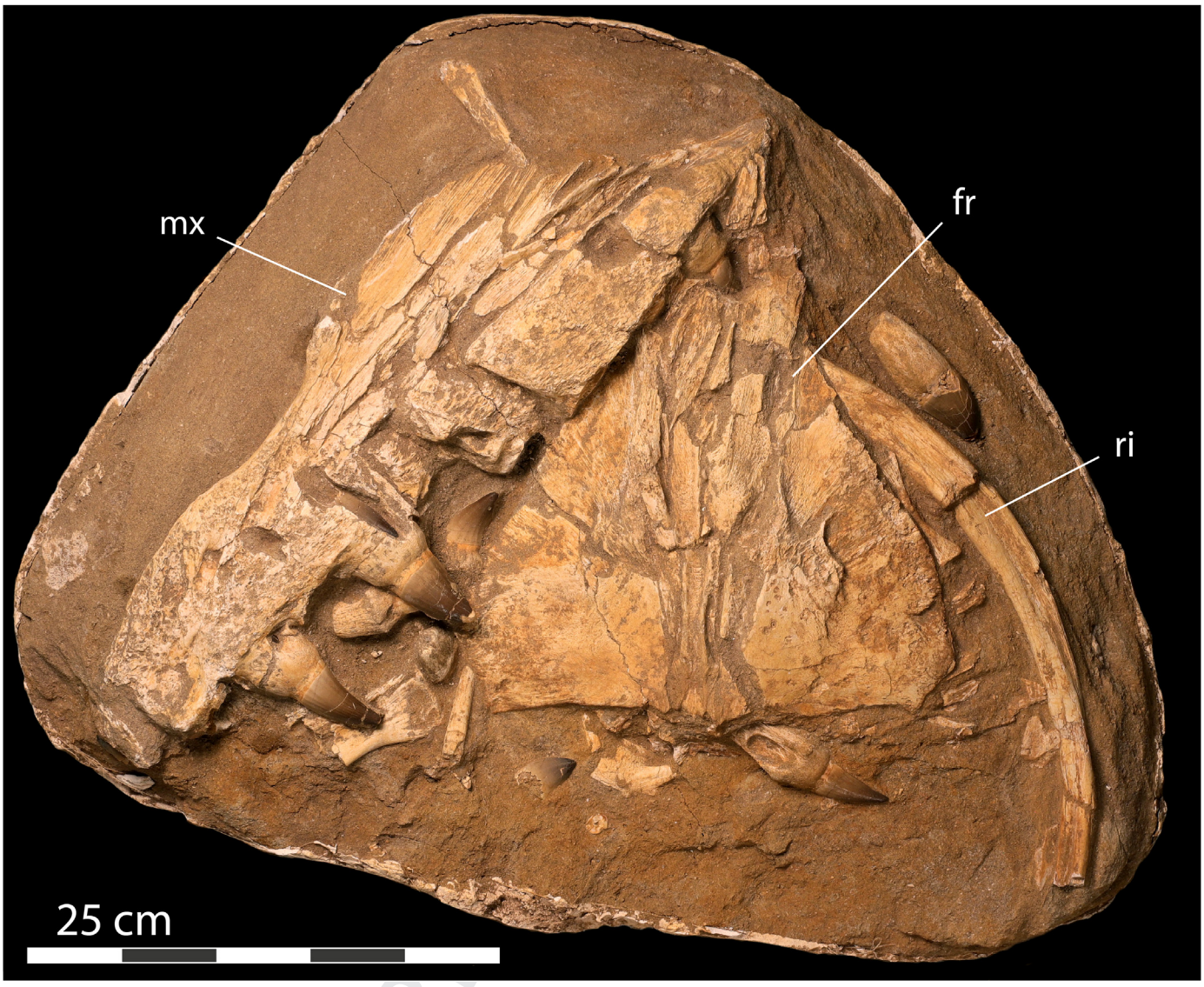

Fig. 11. *Thalassotitan atrox*, referred specimen MHNM.KH.1047, late Maastrichtian age, Upper Couche III of Sidi Daoui, Oulad Abdoun Basin, Morocco. Frontal in ventral view, right maxilla in medial view, and rib. Abbreviations: max, maxilla, fr, frontal, ri, rib.

frontal over the parietal and a broad prefrontal–postorbitofrontal contact above the orbit. Both characters occur in *Thalassotitan*.

Postorbitofrontal. The postorbitofrontal contacts the prefrontal anteriorly, the frontal and parietal medially, the squamosal posteriorly, and the jugal laterally. It has the typical mosasaurid shape, wrapping around the frontal-parietal contact anteriorly, and forming most of the supratemporal fenestra's lateral margin posteriorly. The bone generally resembles other Prognathodontini (Lingham-Soliar and Nolf, 1989; Christiansen and Bonde, 2002; Konishi et al., 2011).

The postorbitofrontal broadly underlaps the frontal's lateral wing, with a slight dorsal exposure where it contacts the prefrontal. The postorbitofrontal-prefrontal contact excludes the frontals from the orbital rim. The postorbitofrontal's orbital margin is rugose. Its lateral margin bears a sharp corner. A short, triangular postorbital process extends ventrally. It forms the posterodorsal margin of the orbit, and its tip would have contacted the jugal. Medially, a long, slender squamosal process of the postorbitofrontal extends behind the parietal, contributing to the lateral margin of the supratemporal fenestra. It broadly contacts the medial surface of the squamosal, forming much of the lateral margin of the supratemporal fenestrae. It tapers posteriorly, with a sharp tip fitting into a V-shaped notch in the squamosal. It ends anterior to the posterior end of the supratemporal fenestra.

Parietal. The fused parietals form an H-shaped element contacting the frontals anteriorly, the postorbitofrontal anterolaterally, and the squamosal and supratemporal posterolaterally, as in other mosasaurids (Russell, 1967). The parietal broadly contributes to the supratemporal fossae, forming its anteromedial, medial and posteromedial margins.

The parietal table is small. It has a narrow contact with the frontals anteriorly, then expands posteriorly so that the parietal table is diamond-shaped. A small, diamond-shaped parietal table also occurs in *P. saturator* (Schulp, 2006) and perhaps in *P. currii*, but not in *P. solvayi* (Lingham-Soliar and Nolf, 1989) or *P. overtoni* (Konishi et al., 2011) where it is larger and triangular. The anterior end of the parietal table fits into a small embrasure made by the posteromedial flanges of the frontal.

Fig. 12. *Thalassotitan atrox*, referred specimen MHNM.KH.326, late Maastrichtian age, Upper Couche III of Sidi Daoui, Oulad Abdoun Basin, Morocco. A, left maxilla and dentary; C, dentary showing healing bone; D, maxilla showing broken and worn tooth exposing pulp cavity.

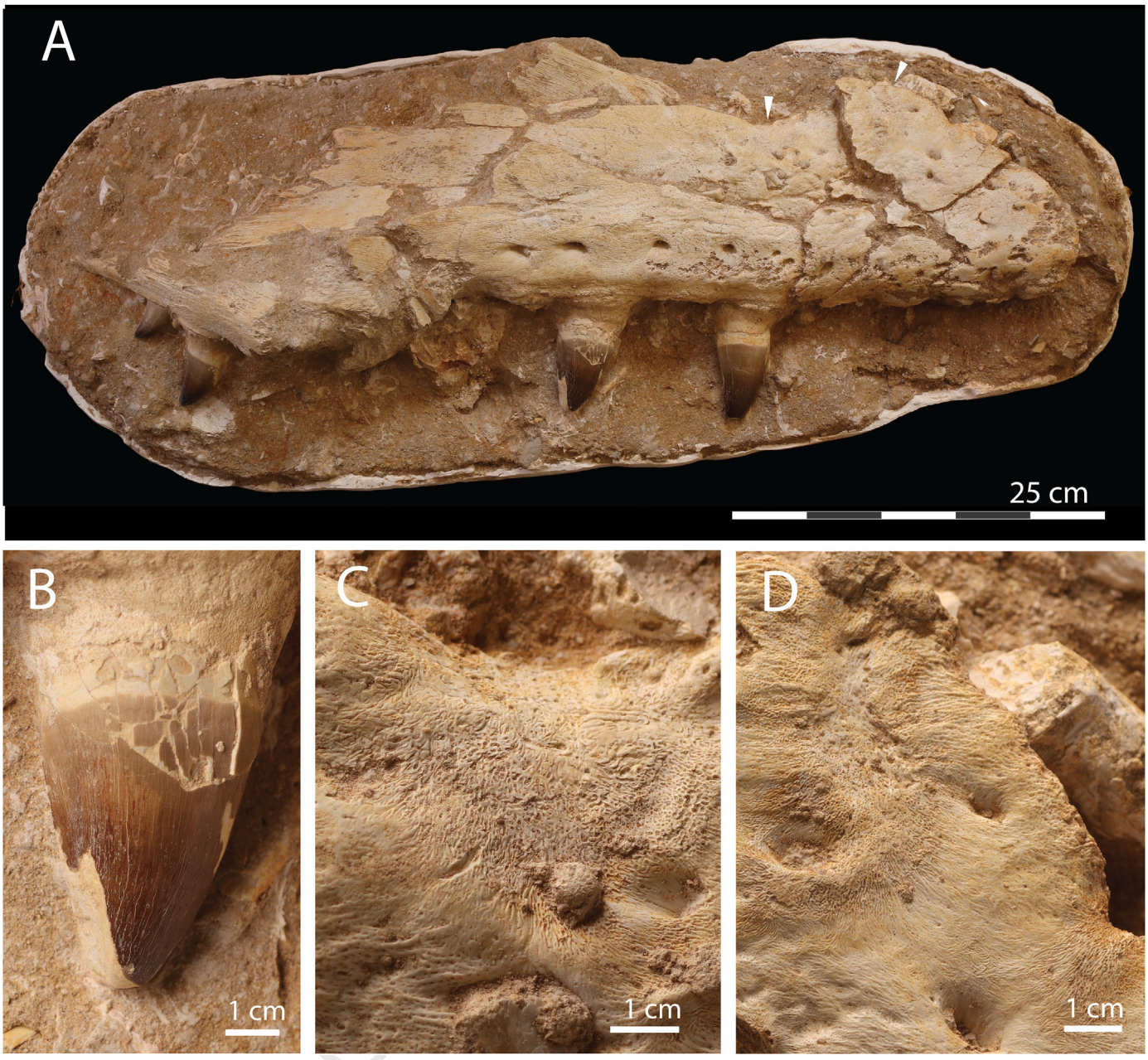

Fig. 13. *Thalassotitan atrox*, referred specimen MHNM.KH.396; late Maastrichtian age, Upper Couche III of Sidi Daoui, Oulad Abdoun Basin, Morocco. A, right maxilla; B, closeup showing tooth damage; C, D, pathological bone texture.

Anteriorly, the pineal foramen lies near the frontoparietal suture. The parietal table completely encloses the pineal foramen, except for a small slit extending forward to the frontoparietal suture. The pineal foramen is small and elongate, as in *P. saturator* (Schulp, 2006).

Behind the parietal table, the parietal narrows. The parietals define the entire medial surface of the supratemporal fossae, with the dorsal rim of the fossae projecting up above the midline of the parietal. The margins of the supratemporal fossae converge so that the supratemporal fossae almost meet to form a sagittal keel in the middle. This condition occurs in *P. saturator*, and perhaps in *P. currii*, but not in *P. solvayi* or *P. overtoni* (Christiansen and Bonde, 2002; Schulp, 2006). A narrow parietal midline also occurs in *Globidens* (Bell, 1997). This probably expands the supratemporal fenestra to increase the area of insertion for jaw adductor muscles, and thus force production (Frey et al., 2001). Broad ventral flanges of the parietal appear to extend downward, but are crushed and broken. The parietal's anterolateral processes have an expanded, crescent-shaped anterior margin where its overlaps onto the frontal and forms the anterior margin of the supratemporal fossae. The tip of the anterolateral processes is notched to receive the medial process of the postorbitofrontal.

Posteriorly, the parietal's suspensorial rami diverge and extend posterolaterally, defining the posterior margin of the supratemporal fossae.Their tips contact the squamosal and supratemporal, as is typical of mosasaurids. In contrast to the more arcuate shape seen in *P. solvayi* and *P. overtoni*, the suspensorial rami hook laterally, then are straight along their length, as in *P. currii* (Bonde and Christiansen, 2003). The suspensorial rami appear to be obliquely oriented rather than horizontal (see Bell,

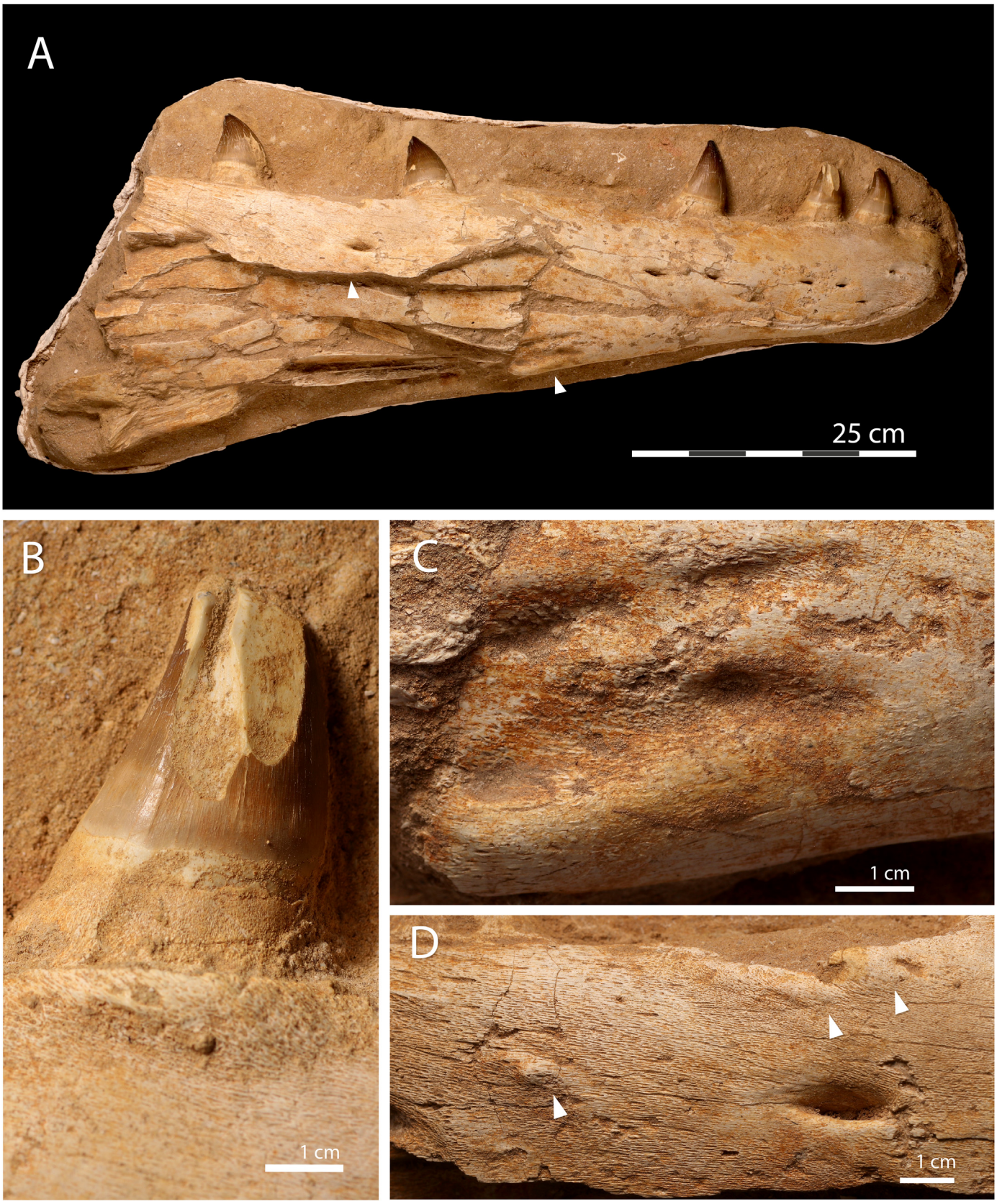

Fig. 14. *Thalassotitan atrox*, referred specimen MHNM.KH.325, late Maastrichtian age, Upper Couche III of Sidi Daoui, Oulad Abdoun Basin, Morocco. A, right dentary; B, spalled tooth crown; C, D, pathological lesion.

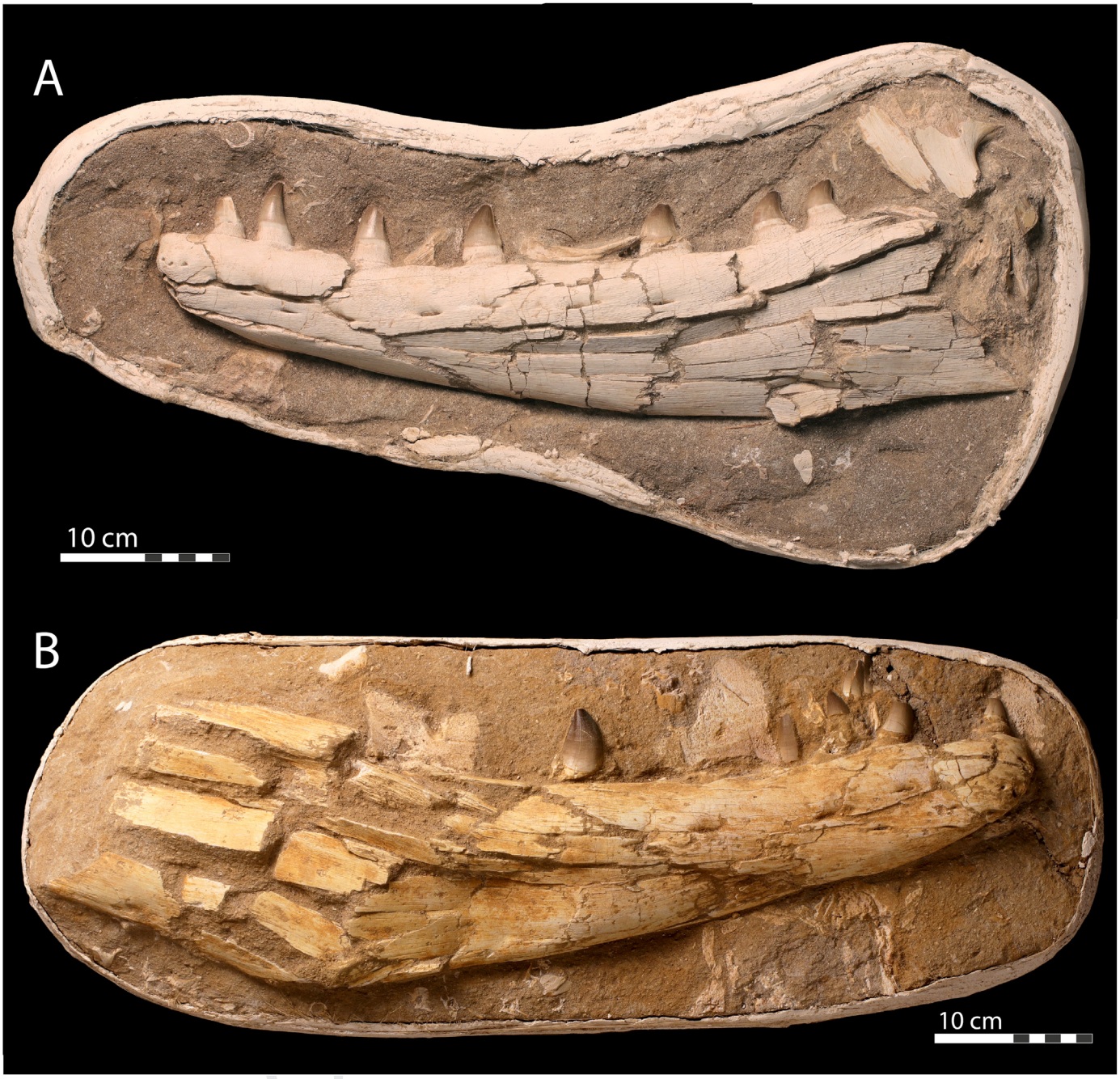

Fig. 15. *Thalassotitan atrox*, juveniles. A, referred specimen MHNM.KH.330, left dentary, late Maastrichtian age, Upper Couche III, Sidi Chennane, Oulad Abdoun Basin, Morocco. B, referred specimen MHNM.KH.1253, right dentary, late Maastrichtian age, Upper Couche III, Sidi Daoui, Oulad Abdoun Basin, Morocco.

1997). They form the skull's posterior margin, giving it a broad V-shape.

Supratemporal fenestrae. The supratemporal fenestrae are large, about a quarter of the skull length. They are roughly triangular, being broad anteriorly and tapering posteriorly. The fenestrae are bordered by the parietal, which contributes to more than half to them, and by the frontal, postorbitofrontal, squamosal and supratemporal.

Squamosal. The V-shaped squamosals form the posterolateral corner of the mosasaurid skull. They contact the parietal medially, the postorbitofrontal anteriorly, and the quadrate and supratemporal ventrally. They also contribute to the posterolateral margin of the supratemporal fossae. The anterior ramus of the squamosal, with the postorbitofrontal, forms the upper temporal bar. The anterior ramus is elongate, extending almost the full length of the upper temporal bar. It forms most of the bar's lateral surface; the postorbitofrontal makes most of its medial surface. The anterior ramus has a V-shaped slot where it embraces the posterior end of the postorbitofrontal, and a sharp dorsal edge delimiting the lateral margin of the supratemporal fossa.

Supratemporal. The supratemporal is weakly exposed in dorsal view in MNHM.KH.231 and in OCP DEK-GE 497 as a slender splint between the right squamosal and the suspensorial ramus of the parietal. It would have contacted the opisthotic and the prootic proximally. Distally it contacted the parietal, squamosal, and quadrate.

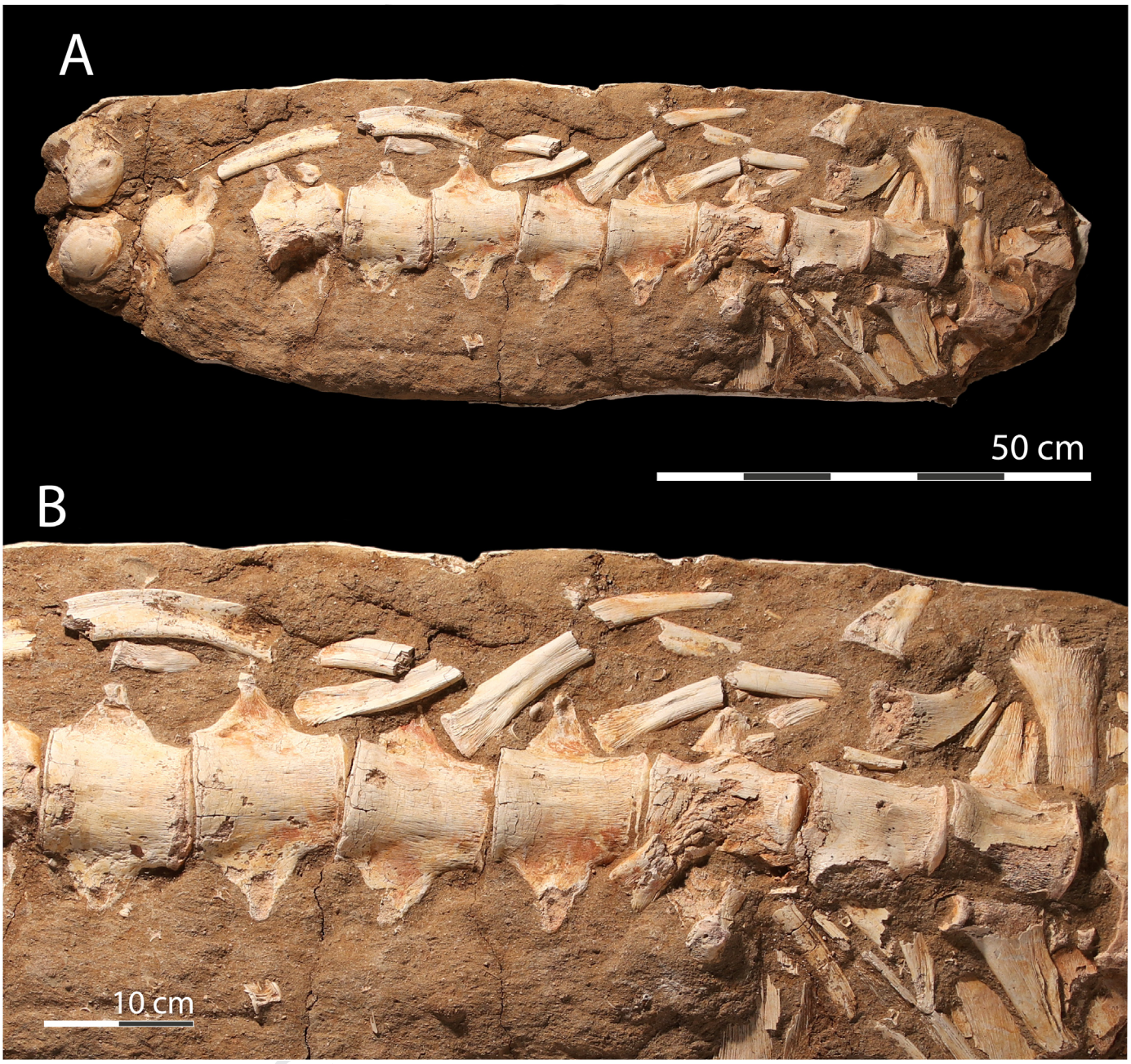

Fig. 16. *Thalassotitan atrox*, referred specimen MHNM.KH.1051, dorsal vertebrae and ribs, late Maastrichtian age, Upper Couche III, Sidi Daoui, Oulad Abdoun basin, Morocco. A, vertebrae and ribs in ventral view; B, closeup.

Quadrate. The quadrate is preserved in several specimens (MNHM.KH.231 and OCP DEK-GE 417, OCP DEK-GE 10, OCP DEK-GE 109). It is a short, massive bone that articulates with the squamosal and supratemporal dorsally, and the glenoid fossa of the mandible ventrally. It is subrectangular, with its height slightly larger than its anteroposterior width. The quadrate's stout construction is similar to that of *P. saturator*, *P. overtoni*, *P. solvayi* (that of *P. currii* is damaged complicating comparisons) and *Globidens* (Russell, 1975). The lateral conch is relatively small and subcircular, its diameter being about half the height of the bone, as in other Prognathodontini and Globidensini. As in *P. saturator* (Schulp, 2006), the conch's anterior margin is massively constructed.

There is a long, robust suprastapedial process; its length exceeds half the quadrate's height. The suprastapedial process's distal end is strongly expanded, being more than twice the width of the process proximally. A similar condition occurs in many Mosasaurinae, e.g. *Gnathomortis stadtmani* (Lively, 2020), *Eremiasaurus heterodontus* (LeBlanc et al., 2012), *Globidens* (Russell, 1975) and *P. kianda* (Schulp et al., 2008), but *P. saturator* lacks this strong transverse expansion (Dortangs et al., 2002). A large oval depression is present on the end of the suprastapedial process, as in *P. overtoni* (Konishi et al., 2011). The suprastapedial process broadly contacts and fuses with a massive, rugose infrastapedial process well below the middle of the bone, contrary to some Prognathodontini (*P. solvayi*, *P. saturator*) in

which these processes fuse near the middle of the shaft. The suprastapedial and infrastapedial processes together define a large tympanic meatus as in other Prognathodontini.

The distal condyle is broad, massive and ovoid. It is transversely convex, similar to *P. saturator* and other Prognathodontini and Mosasaurinae in general (Lingham-Soliar, 1995; Schulp, 2006), suggesting the ability to rotate the mandibles about their long axes.

Laterally, the quadrate bears a large tympanic ala that is expanded anteroposteriorly to create a large lateral conch as typical of mosasaurids. Medially, there is a stapedial pit on the medial surface of the quadrate above the otic notch; it is large and almost circular.

Pterygoids. The pterygoids are typical of mosasaurids (except *Globidens*) in bearing a row of pterygoid teeth. As in *Prognathodon saturator*, *P. solvayi*, and *P. overtoni* (Lingham-Soliar and Nolf, 1989; Schulp, 2006; Konishi et al., 2011), pterygoid teeth are massive, approaching the size and shape of the marginal teeth. In the specimens where the pterygoid is preserved, it bears at least 6 teeth.

Basicranium. The basicranium is poorly preserved in most specimens, and only visible clearly in OCP DEK-GE 109. It includes the basiphenoid, basioccipital, prootic and exoccipital-opistothic; here all bones are fused and preserved in right lateral view above the left mandible ramus. It is very robust and exhibits the general traits of mosasaurid basicranium (Russell, 1967).

The basisphenoid has a typical square shape. Anteriorly it bears a long, slender parasphenoid rostrum and large, rounded basipterygoid processes, well separated from the main shaft. A large concave notch separates the basipterygoid processes. Posteriorly the basisphenoid abuts the basioccipital via a long ala of bone that anchors the basal tubera. Dorsally, the suture with the prootic and the opistothic-exoccipital is long and posteroventrally transversely oriented. Laterally, the Vidian canal is visible and the channel for the jugular vein is widely open, probably because the dorsal ala of the basisphenoid is broken.

Posteriorly, the basioccipital projects dorsoposteriorly to form a convex occipital condyle. Ventrally, large ventral basal tubera with convex extremities are seen. Both are separated by a neck. The basioccipital contacts anteriorly the basisphenoid in a transversly antero-descending straight suture.

The prootic is a triradiate bone as typical of mosasaurids. The anterior ascending ramus is crushed. The descending anterior ramus is large. Its suture with the basisphenoid is small and transversely oriented, whereas the one for the opistothic-exoccipital is long and almost vertical. The otosphenoidal crest is poorly developed, such that it does not conceal the foramen for the cranial nerve VII. The posterior ascending ramus is long and narrow, with straight margins. It bears strong longitudinal striae and is loosely sutured over the paroccipital process of the opistothic.

The opistothic-exoccipital is fused as in other mosasaurids (Russell, 1967). It contacts the basipshenoid and basioccipital ventrally, the prootic laterally, and the suspensorium dorsally. The exoccipital appears as a square bone abutting the dorsal surface of the basioccipital in a transverse anteriorly descending suture. Ventrally, the opisthotic-exoccipital has a thin descending lamina of bone that covers most of the basioccipital lateral surface above the basal tubera; this lamina appears to contact the basisphenoid in a large transverse suture like in *Mosasaurus* (Lingham-Soliar, 1995) and *P. solvayi* (Lingham-Soliar and Nolf, 1989). The lateral surface is poorly preserved and the foramina for cranial nerves XII, IX, X and XI are not visible. Only the internal auditory meatus is visible, dorsal to the exit for cranial nerve VII. Dorsally, the paroccipital processes are long, large and end in a fan-shape. Like the prootic, the paroccipital processes bears strong longitudinal striae on their lateral and medial surfaces.

Mandible

Dentary. The dentary is a robust bone, contacting the splenial medially, and the surangular, prearticular and coronoid posteriorly. The dentary is relatively deeper than in *P. solvayi* or *P. overtoni*, but less robust than in *P. currii*; in proportions it closely resembles *P. saturator*. The dentary has 14 tooth positions, as in *P. saturator* (Schulp, 2006); *P. solvayi* has 13 (Lingham-Soliar and Nolf, 1989), and *P. currii* has 12 (Christiansen and Bonde, 2002).

The tip of the dentary is bluntly rounded, but lacks a predental prominence, as in other Prognathodontini. In other mosasaurines, e.g. *Mosasaurus hoffmanni* (Lingham-Soliar, 1995), a predental prominence extends well ahead of the first tooth.

In lateral view, the dentary is strongly bowed as in other Prognathodontini, with a concave dorsal margin and a convex ventral one. A row of large neurovascular foramina lies low on the lateral surface of the dentary and runs along its length. They are small and closely spaced anteriorly, and larger and widely spaced posteriorly. Medially, a tall subdental lamina forms the medial wall of the tooth sockets, so that the medial and lateral parapets lay at the same level, as typical of Mosasaurinae (Lingham-Soliar and Nolf, 1989; Lingham-Soliar, 1995; Schulp et al., 2008). The Meckelian canal extends to the dentary tip and is deep and broad posteriorly.

The posterior margin of the dentary is oblique and lacks an edentulous process behind the last tooth. There is a deep slot just below the last tooth, as in other mosasaurines (Lingham-Soliar, 1995; Schulp, 2006), which may have received the tip of the coronoid. Ventrally it ends in a sharp corner like in *P. overtoni* (Konishi et al., 2011) and *Mosasaurus*. Posteriorly, the dentary contacts the coronoid and surangular. The contacts were loose, contributing to a mobile intramandibular joint.

Splenial. The splenial contacts the dentary's medial and ventral surfaces, the prearticular posteriorly, and the angular posteroventrally. Medially, the splenial has a large triangular wing covering the dentary and extending up to the subdental lamina. This medial wing is expanded anteriorly, covering up to three-quarters of the dentary and the Meckelian canal. Posteroventrally, it bears a large oval foramen. Ventrally, the splenial projects below the dentary to become visible in lateral view, as is typical of mosasaurids. It tapers to disappear from lateral view below the fourth tooth like in *Prognathodon*. Posteriorly it extends slightly past the dentary's posterior margin, as in *P. solvayi* (Lingham-Soliar and Nolf, 1989). The articulation with the angular is oval and bears a median ridge. It formed a mobile articulation, contributing to the intramandibular joint.

Coronoid. The coronoid is a large, saddle-shaped bone. It contacts the dentary anteriorly, and articulates with the surangular's dorsal, lateral, and medial surfaces.

The coronoid's dorsal wing is a tall, triangular process contributing to a well-developed coronoid process and adductor fossa. It closely resembles *Prognathodon saturator*, *P. solvayi*, *P. lutugini*, and *P. overtoni* (Schulp, 2006; Grigoriev, 2013) in having a sharp, narrow apex, and in being posteriorly extended to form a large part of the coronoid process' dorsal margin. In *Mosasaurus*, the apex of the coronoid process is blunter (Lingham-Soliar, 1995; Street and Caldwell, 2017), and the posterior ala is shorter, making a limited contribution to the posterodorsal margin of the coronoid process.

The coronoid's anterolateral margin bears a small notch and longitudinal striations. The coronoid's ventrolateral wing forms a deep, semicircular flange that extends down to broadly cover the surangular. A similar flange occurs in *P. saturator* (Schulp, 2006); that of *P. solvayi* (Lingham-Soliar and Nolf, 1989) and *P. overtoni* (Konishi et al., 2011) is smaller, and the ventral flange of *Mosasaurus hoffmanni* is much smaller (Lingham-Soliar, 1995; Street and Caldwell, 2017). In medial view, an anteromedial wing extends down the inside of the surangular to reach the angular. It is broad and deep, as in other Mosasaurinae.

UNCORRECTED PROOF

Surangular. The surangular contacts the dentary anterolaterally, the splenial anteromedially, the coronoid dorsally, the prearticular medially, the angular ventrally, and the articular posteriorly. It is a large, triangular and robust element occupying most of the posterior mandible's lateral surface. The surangular is deep anteriorly and shallower toward the back of the jaw.

The surangular's dorsal wing makes a large contribution to the coronoid process, but as in other Prognathodontini, it lacks the tall, triangular dorsal wing seen in *Mosasaurus* (Lingham-Soliar, 1995). The dorsal margin of the ascending wing is convex, whereas it is concave in *P. saturator* and *P. solvayi*; there is a very slight convexity in *P. overtoni* (Lingham-Soliar and Nolf, 1989) (Schulp, 2006; Konishi et al., 2011). The condition is unknown for *P. currii*.

Laterally, the surangular is broadly exposed ventral to the coronoid, and its surface is slightly convex. The anterior contact with the dentary is sigmoid and the lateral suture with the angular and articular is nearly straight, becoming convex posteriorly at the level of the glenoid fossa. Posteriorly, the surangular's dorsal margin is concave where it contributes to half of the glenoid fossa.

Angular. The angular is a long, triangular bone. It contacts the splenial anteriorly in a strongly convex oval articulation, and the surangular and prearticular dorsally. Laterally, it has a very small triangular exposure anteriorly where it joins the splenial, and ventrally along a straight suture that runs the entire length of the surangular. The medial wing is weakly expanded dorsally.

Articular-prearticular. The prearticular and articular are fused as in other mosasaurids (Russell, 1967). Medially, the articular-prearticular complex forms an elongate tongue contacting the splenial anteriorly, the coronoid anterodorsally, the surangular dorsally, and the angular ventrally.

The articular's contact with the splenial is mobile and helped form the intramandibular joint, allowing the mandible to hinge outwards. The medial suture with the surangular is concave, while the lateral contact is nearly straight except in its posterior part, where it becomes concave near the glenoid fossa. Posteriorly, the articular forms the medial half part of the glenoid. The glenoid is strongly concave, as in *P. saturator*, *P. solvayi*, and *P. overtoni* (Schulp, 2006); *M. hoffmanni* has a shallower glenoid (Lingham-Soliar, 1995; Street and Caldwell, 2017). Posteriorly, the retroarticular process is robust, almost rectangular, and horizontally oriented. Its ventral margin is concave where the retroarticular process is ventrally deflected, as in other Mosasaurinae.

Dentition

Tooth crowns are large and robust, roughly conical in shape, and weakly curved. Teeth resemble those of *P. saturator* (Dortangs et al., 2002), but differ in being slightly shorter, and more robust. The crowns are slightly swollen basally, as in *P. saturator* and *P. overtoni* (Konishi et al., 2011), but they lack the rounded shape seen in *P. currii* (Christiansen and Bonde, 2002; Bardet et al., 2005a). The most striking differences are observed with *P. solvayi* (Lingham-Soliar and Nolf, 1989), in which the teeth bear numerous ridges.

The labial and lingual surfaces of the crowns are smooth, as in *P. saturator* (Schulp, 2006) and *P. giganteus* (Lingham-Soliar and Nolf, 1989). They lack the facets or prisms seen in *Mosasaurus hoffmanni* (Lingham-Soliar, 1995; Street and Caldwell, 2017) and *M. beaugei* (Bardet et al., 2004) or the prominent ridges seen in *P. solvayi* (Lingham-Soliar and Nolf, 1989). However, the tooth's medial surface sometimes bears subtle ridges. The development of these ridges is highly variable, varying even along the tooth row, and occurring in some specimens but not others, suggesting individual and/or ontogenetic variation.

At the crowns' apex, the enamel is ornamented with coarse bumps and anastomosing ridges. Similar texture occurs in other Prognathodontini, including *Prognathodon solvayi*, *Prognathodon giganteus* (Lingham-Soliar and Nolf, 1989), *Prognathodon lutugini* (Grigoriev, 2013), *Prognathodon currii* (Christiansen and Bonde, 2002), as well as *Globidens* spp. (Gilmore, 1912; Bardet et al., 2005a) and *Carinodens belgicus* (Schulp et al., 2009). Ornament is restricted to the apex of the tooth in *T. atrox*, *P. solvayi* (NRL pers. obs.) and *P. lutugini*. In *P. currii*, *Globidens* (Bardet et al., 2005a) and *Carinodens* (Schulp et al., 2009) the ornamentation extends halfway down the crown or more.

Carinae are well-developed. The anterior carina is typically more convex, and the posterior carina more weakly curved, or straight. On the anterior teeth, the anterior carina extends the whole height of the crown, whereas the posterior one is displaced posterolingually and developed only on the upper third of the crown. On middle and posterior teeth, carinae are aligned anteriorly and posteriorly so that the crown's labial and lingual surfaces are equal in size. Posterior carinae in these teeth are pronounced, and project to create a strong cutting edge. This prominent, blade-like posterior carina occurs in other Prognathodontini (Lingham-Soliar and Nolf, 1989), *Mosasaurus* (Lingham-Soliar, 1995), and *Clidastes* (Lindgren and Siverson, 2004).

Anterior and posterior carinae bear fine denticulations. Serrations are variably developed in Mosasaurinae. They are present in *P. saturator*, *P. currii*, *P. lutugini* (Grigoriev, 2013), *P. solvayi*, *M. hoffmanni* (NRL pers. obs.), *Eremiasaurus heterodontus* (LeBlanc et al., 2012); serrations are absent in *P. kianda* (Schulp et al., 2008).

Teeth implant into discrete sockets delimited by interdental ridges, as typical of Mosasauridae (Rieppel and Kearney, 2005; Luan et al., 2009). Roots are huge and barrel-shaped, as in *Mosasaurus* (Lingham-Soliar, 1995), being much fatter and longer than the crowns, and protruding above the alveoli to form a huge pedicel. Replacement teeth form in deep subdental crypts within the root, as is typical of derived mosasaurids (Rieppel and Kearney, 2005; Luan et al., 2009).

Dentary teeth are more laterally compressed than maxillary teeth. Marginal teeth also show well-developed heterodonty, as in other Mosasaurinae (Lingham-Soliar and Nolf, 1989; Lingham-Soliar, 1995; LeBlanc et al., 2012). The teeth change in size, shape, and curvature along the toothrow. The first 4–5 teeth are narrow and high, with circular basal cross-sections, and are weakly procumbent, but less so than in *Prognathodon solvayi* (Lingham-Soliar and Nolf, 1989). Succeeding teeth are larger and more robust, more erect, and have a lenticular basal cross-section. The last few teeth are smaller again, proportionately as broad as tall, and laterally compressed, their basal cross-section being narrowly lenticular. Tooth curvature varies along the toothrow. Teeth are weakly recurved in the middle of the tooth row, with a convex anterior surface and a nearly straight to weakly concave posterior one. They become more strongly curved posteriorly; the last teeth are sharply hooked, like the pterygoid teeth.

Pterygoid teeth are large and robust, almost reaching the size of the marginal teeth, as in other Prognathodontini and in *Plesiotylosaurus* (Bell, 1997).

Postcranial skeleton

Postcranial elements are preserved on the syntypes MNHM.KH.231 (cervical and dorsal vertebrae, ribs), OCP DEK-GE 417 (cervical and dorsal vertebrae, ribs, pectoral girdle and forelimb), and referred specimens OCP DEK-GE 109 (cervical and dorsal vertebrae, ribs), OCP DEK-GE 90 (cervical vertebrae) and OCP DEK-GE 497 (isolated limb elements).

UNCORRECTED PROOF

Vertebrae

Vertebrae are procoelous, with deeply cupped anterior cotyles and large, convex posterior condyles. They resemble other Mosasaurinae. The cervical series preserves the atlas neural arch, axis, and vertebrae C3-7. Their centra are slightly wider than long. The atlas neural arch bears the typical square to triangular shape with a long, posteroventrally positioned synapophyseal process. The axis has a tall, robust neural arch, an intercentrum with a large process, and a large oval hypapophyseal peduncle.

Cervicals 3 to 7 bear heart-shaped articular surfaces that become round in the last cervicals. Neural spines increase in size along the series, measuring up to 20 cm in C7 of OCP DEK-GE 109. Cervical pre- and postzygapophyses are large, and widely spaced. The zygosphene–zygantrum complex is also enlarged. Cervical synapophyses are large, robust, and located anterodorsally on the centrum. They are rounded in cross-section in anterior cervicals, and become reniform in cross-section in posterior ones, being as wide as the centrum itself. Short, very robust, round to oval hypapophyses project from the centrum's ventral surface.

Dorsal centra are cylindrical in shape, and slightly longer than wide. Articular surfaces are rounded. Neural spines are high and robust. Transverse processes are large, rectangular and lie anterodorsally on the lateral surfaces of the centra. Pre- and postzygapophyses are large and well developed on the 20 dorsal vertebrae preserved on OCP DEK-GE 417; the zygosphene–zygantrum complex is large. Ribs are short, robust, and strongly curved anteriorly, then become large and weakly curved posteriorly, as typical of mosasaurids.

Pectoral girdle

The pectoral girdle, including both scapulae and coracoids, is preserved on specimen OCP DEK-GE 417. The bones are crushed, but their shapes can be approximated.

The scapula and coracoid are robust and comparable in size. The two bones meet in a loose contact, and the sutural contact between them is wider than the glenoid cavity. The pectoral girdle differs from that of *Clidastes*, *Platecarpus* and *Tylosaurus* (Russell, 1967) and overall resembles that of *P. overtoni* (Konishi et al., 2011) and *Mosasaurus conodon* (Ikejiri and Lucas, 2015), but differs from *Mosasaurus* in having a more square shape for both bones, and in lacking a large coracoid emargination (Ikejiri and Lucas, 2015).

The scapula is squarish in shape, its height and length being subequal. It lacks a well-defined proximal neck, and expands anteroposteriorly to form a convex, fan-shaped blade. Its surface bears marked, radiating striations. The scapula has a short, almost horizontal anterior margin ending in a rounded corner, whereas the posterior one is straight just above the glenoid cavity, then concave, then straight dorsally. The dorsal margin is strongly convex from side to side, giving the bone this squared shape.

The coracoid is very stocky. As with the scapula, it is subquadratic in shape with the height and length subequal, and lacks a well-defined neck. The blade's anterior and posterior margins are weakly concave and similar in length. The ventral margin is strongly convex. As with the scapula, the bone bears radiating striations. The coracoid bears a large foramen located anteroproximally and a broad, deep anterior emargination.

Forelimb

Both forepaddles are preserved disarticulated in OCP DEK-GE 417. Some disarticulated elements also lie behind the skull in OCP DEK-GE 497. OCP DEK-GE 417 preserves both humeri in ventral view, in roughly natural position with respect to the pectoral girdle.

The humerus as a whole is very stocky, roughly as wide as long. The dorsal condyle is convex but does not project dorsally beyond the postglenoid process, contrary to *P. overtoni*. In most mosasaurids, both lie at the same level, or the condyle lies below the postglenoid process (Russell, 1967). Both the glenoid condyle and the postglenoid process appear to be cartilaginous, and are separated from the main shaft of the bone by a loose suture. It is unclear if they are separated (as in *M. conodon*) (Ikejiri and Lucas, 2015) or continuous as in *P. overtoni* (Konishi et al., 2011) and *Clidastes* (Russell, 1967). The deltopectoral crest is large and extends posterodistally toward the middle of the shaft, as in *P. overtoni*. It appears continuous with the deltoid process as in *P. overtoni* (Konishi et al., 2011). The postglenoid process is large and rounded. The ectepicondyle is small and rounded whereas the entepicondyle is rounded and larger, being twice the size of the former. The articular facets for radius and ulna are large and form an angle of about 140°; the radial facet is larger than the ulnar one. Except for the proximal expansion of the glenoid condyle beyond the postglenoid process, the humerus is similar to *P. overtoni* (Konishi et al., 2011). It differs from *Mosasaurus* (Lingham-Soliar, 1995) in being more robust and squared.

The right radius lies in articulation with the humerus. It is large, almost as large as the humerus and much larger than the ulna, as usual in mosasaurids (Russell, 1967). It differs from most mosasaurids (where this bone has an hourglass-shape, and a fan-like distal expansion) in having a crescentic to subrectangular shape, with a convex anterior margin, and a concave posterior one. Distally, there are two articulations: one long and straight for the radiale, one tiny and obliquely oriented for the intermedium.

The right ulna remains articulated with the humerus. It has an hourglass shape with the proximal part wider and thicker than the distal end. The distal articulation bears three facets: a small oblique, anterior facet for the intermedium, a median one for the ulnare, and a small posterior oblique one for the pisiform. As a result, the antebranchial foramen would have been rounded, and the radiale and ulnare would be excluded by articulation of the intermedium with the radius and ulna.

The carpal series is fully ossified as in most Mosasaurinae (Russell, 1967). It includes a rectangular radiale, a saddle-shaped intermedium, a square ulnare, and three more or less rectangular to square distal carpals (preserved on OCP DEK-GE 417 but also on OCP DEK-GE 497). A pisiform is probably present based on the articular surface found on the ulna, but cannot be identified here.

The metacarpals are intermediate in shape between the slender metacarpals of *Clidastes* and the stouter metacarpals of *Mosasaurus* (Russell, 1967; Ikejiri and Lucas, 2015). The metacarpals' proximal ends are larger and thicker than the distal ends. Their proximal margin is more deeply concave than the distal one. As usual, metacarpal I is twice as wide as metacarpal II. The anterior margin of metacarpal bears two processes, one at the metacarpal's base, and one at the tip. Similar processes occur on metacarpal I of other Mosasaurinae, including *Mosasaurus* (Lingham-Soliar, 1995), *Plotosaurus* (Lindgren et al., 2008), and *Carinodens* (Kaddumi, 2009).

The phalangeal formula is unknown, but there were probably 5 digits as in other mosasaurids, with first digit being the most robust. Manual phalanges are strongly hourglass shaped, but they are much more elongate than the short, stout phalanges in Mosasaurini such as *Mosasaurus* and *Plotosaurus*, or in *Carinodens*. Phalanx I-1 bears the same anterior processes found on metacarpal I, but these processes are absent on more distal phalanges. Anterior processes are absent from digit I in *Clidastes* (Russell, 1967). In

UNCORRECTED PROOF

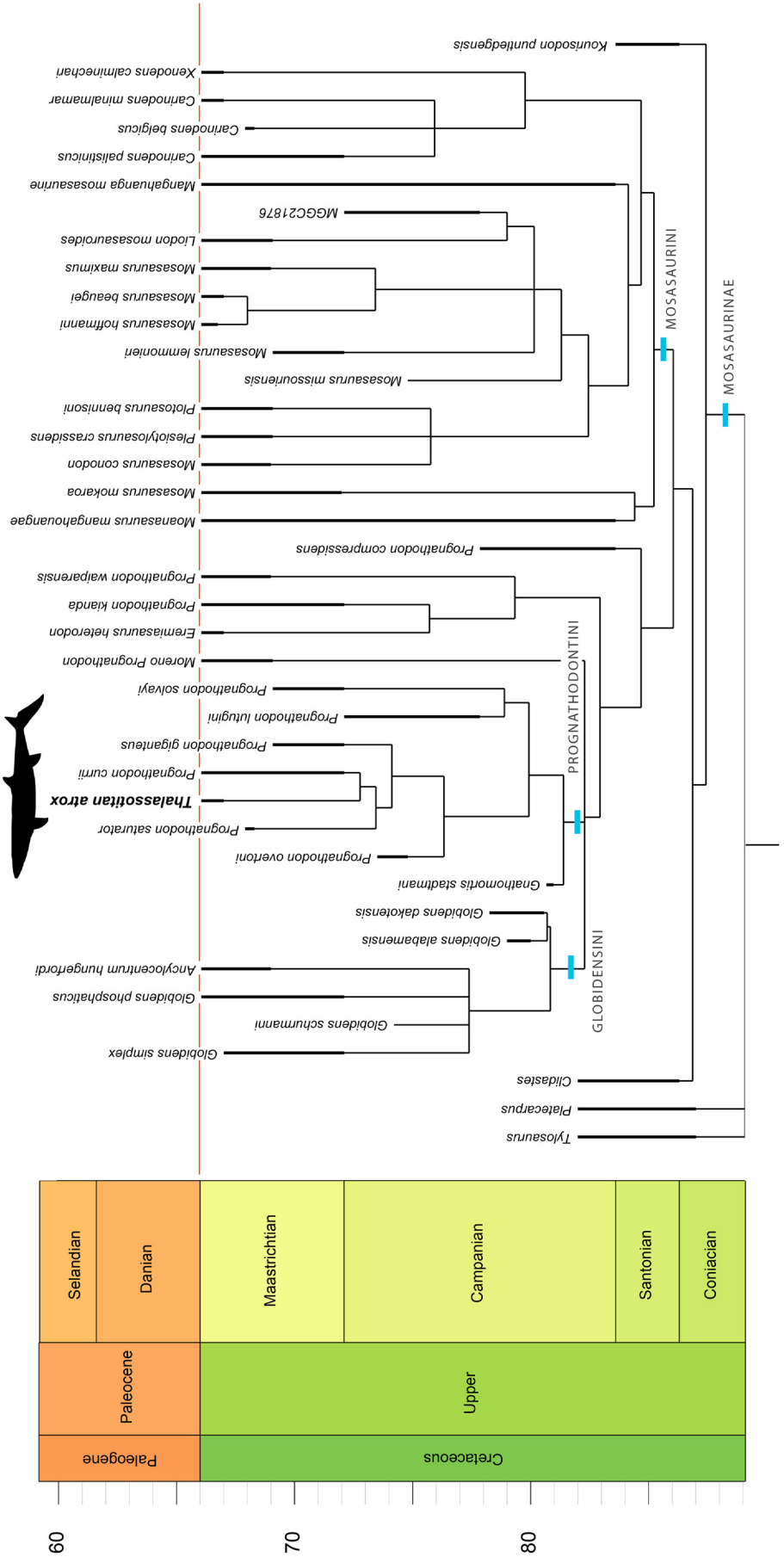

Fig. 17. Phylogenetic analysis of Mosasaurinae, showing the position of *Thalassotitan atrox*.

Mosasaurus, *Plotosaurus*, and *Carinodens*, anterior processes occur on phalanx I-1 and on more distal phalanges. There are possibly 5 phalanges in digit I; three are tentatively identified from digit II, and four to digit III but this does not represent the complete phalangeal series. *Platecarpus* has three phalanges in digit I (Konishi et al., 2012). Mosasaurini have a higher phalangeal count: *Mosasaurus* has 9 phalanges in digit I (Lingham-Soliar, 1995), *Plotosaurus* has 10 (Russell, 1967). The terminal phalanges are rounded distally, lacking the ungual.

Overall the forelimb resembles that of Mosasaurini (Lingham-Soliar, 1995; Lindgren et al., 2008), but was more primitive, having fewer and more elongate phalanges, which lack anterior processes distally. The paddle is longipinnate, but little more can be said of its shape.

3. Phylogenetic analysis

Phylogenetic analysis was conducted using a new character-taxon matrix with characters and taxon-sampling targeting Mosasaurinae (Fig. 17). The matrix includes 113 morphological characters and 38 taxa, with *Platecarpus* and *Tylosaurus* as outgroups. Analysis was conducted using PAUP* 4.0b10 (Swofford, 2002). Stratigraphy was incorporated as an ordered, irreversible character, arbitrarily downweighted to 0.1% of a morphological character to act as a tiebreaker to choose between the shortest trees found on the basis of morphology. Analysis recovered 324 shortest trees (tree length = 337; consistency index = 0.4184; retention index = 0.7131; rescaled consistency index = 0.2983).

Within Mosasaurinae, three major clades are recovered: Mosasaurini, Globidensini, and Prognathodontini. All three clades have been proposed before, but their membership found here is distinct. *Thalassotitan atrox* is part of Prognathodontini and sister-taxon to *Prognathodon currii*. Then *Prognathodon saturator*, *Prognathodon giganteus*, *Prognathodon overtoni*, and a *P. solvayi* − *P. lutigini* clade form successive outgroups. This membership is broadly similar to Russell's (1967) Prognathodontini with the exception that *Plesiotylosaurus* is recovered within Mosasaurini.

One of the main result of our analysis is that, as in previous works (LeBlanc et al., 2012; Simões et al., 2017; Lively, 2020), taxa previously referred to *Prognathodon* fail to form a monophyletic clade. Other analyses have recovered *Prognathodon* as part of a clade with *Globidens* to the exclusion of *Mosasaurus*. We recovered a sister-group relationship between Globidensini (including the fragmentary *Ancylocentrum hungerfordi*) and Prognathodontini. *Prognathodon kianda* and *Prognathodon waiparensis* were not recovered within Prognathodontini but, with *Eremiasaurus heterodontus*, as sister-group of the *Globidens*-*Prognathodon* clade. "Aff. *Prognathodon overtoni*" from the Maungataniwha Sandstone of New Zealand (Wiffen, 1990) is here recovered as a basally diverging mosasaurine. *Carinodens* and *Xenodens* are allied with Mosasaurini, not Globidensini, as previously suggested (Longrich et al., 2021b).

Within the Prognathodontini, *Gnathomortis stadmani* is recovered as a basally diverging lineage. In the Campanian, two main lineages emerged. One gives rise to a clade formed by *P. solvayi* and *P. lutugini*. This clade is characterized by small size and a reduced tooth count, with 13 dentary teeth, and a highly procumbent first dentary tooth. The other lineage gives rise to *Thalassotitan atrox*, *P. currii*, and *P. saturator*. This clade is characterized by large size, massive teeth and jaws, and a narrow, diamond-shaped parietal table.

Mosasaurids show high homoplasy, especially in tooth and jaw morphology. This complicates phylogenetic reconstruction because many taxa are based on cranial remains, often fragmentary. Many key specimens are also incompletely described, exacerbating these issues. It seems likely that relationships between *Prognathodon*, *Globidens*, and *Mosasaurus* will continue to shift as more complete remains are found. Accordingly, we propose phylogenetic definitions for these clades sensu Sereno (1998) to create a taxonomic framework that is robust against changes in inferred tree topology.

Prognathontini is here defined as all mosasaurids closer to *Prognathodon solvayi* than to *Globidens alabamensis* or *Mosasaurus hoffmanni*. Globidensini is defined as all mosasaurids closer to *Globidens alabamensis* than *Prognathodon solvayi* or *Mosasaurus hoffmanni*. Mosasaurini is defined as all mosasaurids closer to *Mosasaurus hoffmanni* than *Globidens alabamensis* or *Prognathodon solvayi*.

These results have implications for mosasaurid taxonomy. Numerous species have traditionally been placed into *Prognathodon*. These span ~15 million years and encompass a range of morphologies. Furthermore, our phylogenetic analysis suggests taxa assigned to *Prognathodon* may not be monophyletic. Recognition of *Thalassotitan* as a distinct taxon further complicates the problem. "*Prognathodon*" *currii* and "*Prognathodon*" *saturator* could be either included in *Thalassotitan*, or perhaps as distinct genera. Reassignment of *Prognathodon overtoni* to the genus *Brachysaurana* (Strand, 1926), as *Brachysaurana overtoni* might also be warranted.

Further revision of prognathodontine systematics is needed but well beyond the scope of this paper, as it will require new fossils, anatomical reviews, and a better understanding of the phylogeny. Pending this broader revision and to avoid further confusing the taxonomy of these animals, we provisionally leave all these taxa in *Prognathodon*.

4. Functional morphology of *Thalassotitan*

Thalassotitan exhibits adaptations suggesting a specialized ecology as an apex predator. The animal's large size, massive skull and robust jaws and teeth likely made it a threat to even the largest marine reptiles in the phosphates, including the giant mosasaurid *Mosasaurus beaugei*, the large elasmosaurid *Zarafasaura oceanis*, and the huge sea turtles *Ocepechelon* and *Alienochelys* (Bardet et al., 2017).

First, *Thalassotitan*'s large size suggests it took large prey. In modern toothed whales, prey size correlates with predator size: large whales take large prey (McCurry et al., 2017b). Larger animals both need more food, and can subdue large prey because of their size. Mosasaurids may also have had higher body temperatures and metabolic rates than terrestrial, ectothermic reptiles (Bernard et al., 2010), and increasing their food requirements. A simple way to meet these requirements is to eat bigger prey.

Second, the shape of *Thalassotitan*'s skull and jaws is convergent on that of predators such as the killer whale, *Orcinus orca* (McCurry et al., 2017a), false killer whale, *Pseudorca crassidens* (Owen, 1846), and pygmy killer whale, *Feresa attenuata* (McCurry et al., 2017a). These species have a short, broad, and roughly triangular rostrum, robust lower jaws; teeth are large, conical, and few in number. A similar morphology occurs in the extinct, predatory whale *Livyatan melvillei* (Lambert et al., 2010).

The skull shape in *Thalassotitan* also increased the forces the jaws can exert and withstand. A short rostrum increased the strength of the skull in bending (Gordon, 1978) and increased bite force, by reducing the out-lever of the jaws. A broad skull increases the jaws' strength in torsion, and the short, robust mandibles increase the jaws' strength in both bending and torsion (Gordon, 1978). Another adaptation to increase bite force is the anterior position of the coronoid process, increasing the length of the in-lever of the jaw in closing (Wainwright and Richard, 1995). Furthermore, the long, broad supratemporal fenestrae increase the cross-sectional area of the jaw adductors, increasing the force these muscles could create.

UNCORRECTED PROOF

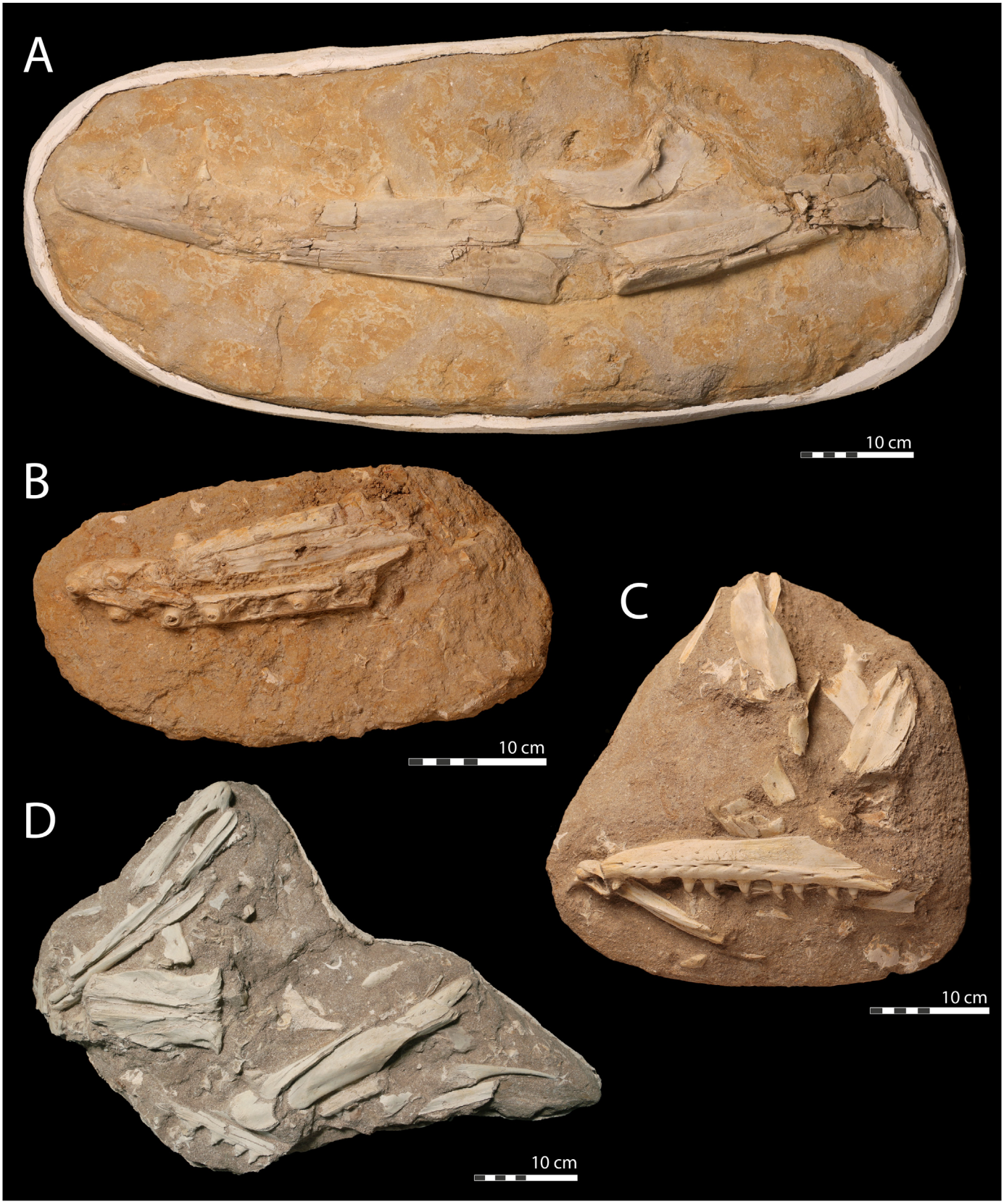

Fig. 18. Mosasaurid remains showing acid damage. A, mandible of *Eremiasaurus heterodontus* MHNM.KH.395. B, rostrum of *Gavialimimus almaghrebensis* MHNM.KH.519; C, partial skull of *Halisaurus arambourgi* MHNM.KH.1259 including maxilla, premaxilla, and surangular; D, Partial skull of *Halisaurus arambourgi* MHNM.KH.1258 including premaxilla, maxilla, and frontals. A–C from upper Couche III, Sidi Daoui; D from upper Couche III, Sidi Chennane.

Fig. 19. Marine vertebrates showing acid damage. A, MHNM.KH.1061, elasmosaurid mandibles, partial skull and atlas; B. *Enchodus libycus*, MHNM.KH.328, acid-damaged jaws found in association with turtle skull, jaws, carapace and phalanges. Both from from upper Couche III, Sidi Daoui.

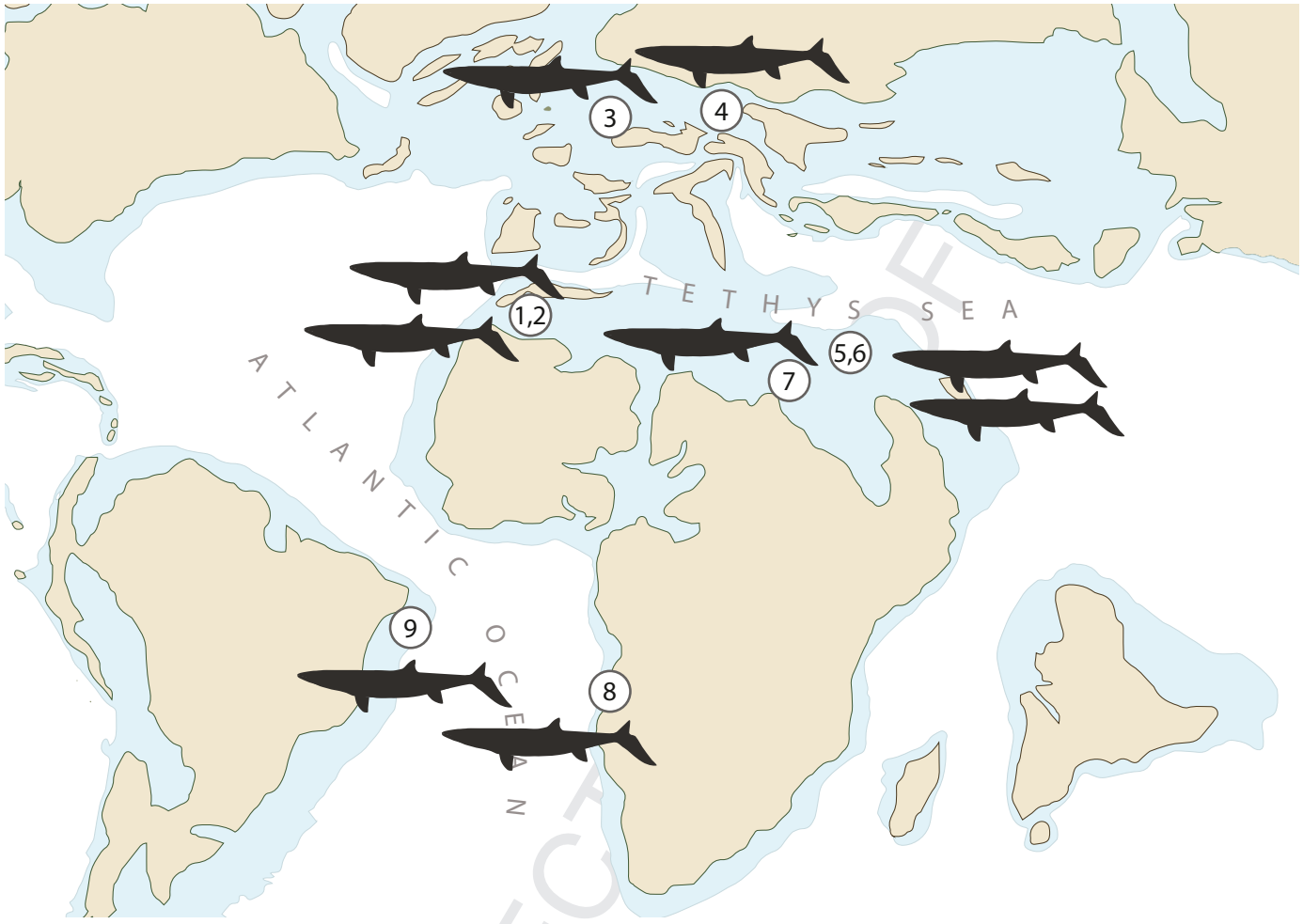

Fig. 20. Distribution of giant carnivorous prognathodontins. 1, Ouled Abdoun Basin, Morocco, *Thalassotitan atrox*, (this paper); 2 Ganntour Basin, Morocco (Cappetta et al., 2014); Ganntour Basin, Morocco, *Thalassotitan atrox* and cf. *Thalassotitan*; 3, Netherlands, *Prognathodon saturator* (Dortangs et al., 2002); 4, Poland (Machalski et al., 2003); 5, Israel (Raab, 1963); 6, Jordan (Bardet and Pereda-Suberbiola, 2002); 7, Egypt (Gemmellaro, 1921); 8, Angola (Schulp et al., 2013a); 9, Brazil (Price, 1957).

Modification of the joints of the skull in *Thalassotitan* also suggests that kinesis was reduced. Among squamates, intracranial and intramandibular kinesis tend to be well-developed (Frazzetta, 1962; Smith, 1980; Arnold, 1988; Herrel et al., 1999). The skull is typically flexible at three points: along the frontoparietal-joint (mesokinetic joint), between parietals and braincase (metakinetic joint) and last, the quadrates can rotate forward (streptostylic joint). In large mosasaurids, kinesis is often reduced to strengthen the skull and increase bite force (Russell, 1967; LeBlanc et al., 2013). In *Thalassotitan*, broad overlap of the parietal onto the frontal, and the frontal onto the parietal, created an interlacing contact that limited movement at the mesokinetic joint. The prefrontals also overlap onto the dorsal surface of the frontal, and interdigitating joints between premaxillae and maxillae, the maxillae and the prefrontals, create a more rigid rostrum. Contrary to the reduced cranial kinetics, the intramandibular joint, allowing a larger gape to swallow large food items, is maintained.

To a degree, this reduced kinesis occurs in other large Mosasaurinae such as *Mosasaurus* and *Plotosaurus* (LeBlanc et al., 2013), but the interlocking condition in *Thalassotitan* is unique in mosasaurids. The closest parallel is perhaps tyrannosaurids, specifically Tyrannosaurini; here tight interlocking between the skull elements minimizes kinesis in *Tarbosaurus baatar* and *Tyrannosaurus rex* (Snively et al., 2006; Cost et al., 2020).

The teeth are also well-adapted to carnivory. In contrast to more basal mosasaurids, *Thalassotitan* has fewer, larger teeth. Reduction in tooth number occurs in *Orcinus orca* and *Livyatan melvillei* (Lambert et al., 2010), and in *T. rex* (Brochu, 2002). Tooth shape resembles that of orcas and *Livyatan*. Strikingly, *Thalassotitan* teeth closely resemble those of 'transient' killer whales (Ford et al., 2011), which specialize in marine mammals, in having short, massive, conical teeth. 'Resident' orcas, which primarily eat fish, have taller, more slender teeth crowns (Ford et al., 2011) like those of *Mosasaurus*. Again, this specialized tooth shape is adapted to resist large forces incurred by biting large prey. The large cross-section of the tooth increases its resistance in bending, torsion, or compression, and the short crowns reduce bending stresses (Gordon, 1978). Finally, the thick anastomosed enamel of the crown increases the resistance of the teeth during handling, biting and shredding of large bony prey (Lingham-Soliar, 1999).

5. Behavioral evidence for the biology of *Thalassotitan*

The abundant specimens of *Thalassotitan*, along with associated fossils, provide a unique opportunity to study the paleobiology of this unusual mosasaurid. Three lines of evidence potentially provide direct evidence of the behavior of this animal. These are (i) tooth wear, (ii) taphonomy of the associated fauna, and (iii)

pathology of the skeleton. Together, these lines of evidence suggest that *Thalassotitan* was a highly aggressive predator that routinely preyed on other marine reptiles, and frequently fought with other members of its species.

Tooth wear

Thalassotitan atrox shows direct evidence for carnivory in the form of tooth wear. Tooth wear is exceptionally heavy, to a degree not seen in any other mosasaurid. Wear is typically seen as large, flat wear facets at the tooth apices, with wear often extending down onto the carinae. Tooth wear is extensively developed in many if not most of the skulls and jaws described here, and in numerous isolated teeth from the Oulad Abdoun Basin (NRL, pers. obs.) and the Ganntour Basin (NB, pers. obs.). Several maxillary and dentary teeth have had their apices broken and were subsequently worn down; both enamel and dentine are worn by use after breakage, showing that this damage occurred in vivo. Apical tooth wear is also heavy in the pterygoid teeth, with apices worn and blunted.

For example, in the skull MHNM.324, of nine teeth, eight show wear, and five show heavy wear, with the apex has been broken or worn away (Fig. 10). Similar wear occurs in a small dentary, MHNM.330 (Fig. 15A). Of 7 preserved teeth, strong wear is seen in six, and two have broken apices. A large dentary, MHNM.325 has five teeth (Fig. 14). Four show modest wear; one has the tip broken and spalled. A large referred dentary and maxilla, MHNM.326 (Fig. 12), has five teeth, and three show little to no wear, one has its apex broken and blunted, and one has the crown broken to expose the pulp cavity, and the dentine is ground and polished. Tooth wear and breakage are also visible on OCP DEK-GE 417 (Fig. 6) and OCP DEK-GE 109 (Fig. 7B).

Tooth wear often occurs in other mosasaurids, for example worn and broken apices in *Mosasaurus hoffmanni* (MNHN AC 9648) and *Pluridens serpentis* (Longrich et al., 2021a), and apical wear in *Globidens* spp. (Bardet et al., 2005a; Martin, 2007) and *Carinodens* (Schulp et al., 2009). Yet in no mosasaurid is tooth breakage and wear as extensive as in *T. atrox*. Heavy tooth wear also occurs in tyrannosaurids (Farlow and Brinkman, 1994; Schubert and Ungar, 2005), including the giant, bone-crushing theropod (Erickson et al., 1996; Longrich et al., 2010; Gignac and Erickson, 2017) *Tyrannosaurus rex*, though not to the degree seen in *Thalassotitan*. Similar levels of tooth breakage and wear occur in hyenas (Van Valkenburgh, 1988), which eat bones and carcasses, but unlike hyenas, mosasaurids replace their teeth (Russell, 1967), so *Thalassotitan* teeth saw comparable levels of wear and breakage even though using them for shorter periods. The degree of tooth wear and breakage implies frequent, high loading against large bones. It is unlikely to result from eating fish, even large fish like *Enchodus*. Instead, it suggests *Thalassotitan* took large bony prey, namely other marine reptiles.

Acid digested fossils

A unique feature of Daoui and Sidi Chennane is an abundance of vertebrate fossils showing decalcification of teeth or damage to bones from acid (Figs. 18–19; SI Figs. 1–6). Acid-damaged fossils represent multiple species, including the mosasaurids *Halisaurus arambourgi*, *Gavialimimus almaghrebensis*, *Eremiasaurus heterodontus*, and an elasmosaurid plesiosaur. Fish such as *Enchodus libycus* and *E. elegans* also show decalcified teeth. Acid-etched teeth of pycnodonts (Cooper et al., 2021) are also found in the assemblage, and have been identified as prey of mosasaurids. In one case, *Enchodus* jaws with decalcified teeth occur directly atop the associated remains of a marine turtle, suggesting it was consumed- and then egested-along with the fish. In the fossils described here, enamel is eaten away (SI Figs. 1–4), along with the underlying dentine of the crown, sometimes exposing the pulp cavity (SI Figs. 2, 3), or even eroding the tooth down to the root (SI Fig. 2). Acid-damaged teeth occur in jaws and skulls, and rarely (if ever) occur among the thousands of shed teeth in the assemblage-including those mosasaurids, plesiosaurs, and sharks. These shed teeth preserve a shiny, pristine enamel layer over the dentine, including shed teeth found centimeters away from jaws showing decalcification. This implies that acidic conditions in the phosphates, before or after burial, did not damage the teeth. Furthermore, since shed teeth are lost by living animals, this implies that decalcification did not occur in *living* animals, either. Instead, tooth decalcification occurred after death, but before burial in decalcified specimens— consistent with their interpretation as animals that have been ingested.

In several specimens, the bone's cortex has been eroded, again consistent with digestion. Although fossils showing decalcification frequently occur in isolation, many are associated elements. Some were sutured in life or tightly held together by strong ligaments, such as the *Eremiasaurus* mandible, and the *Gavialimimus* rostrum (SI Fig. 2) others are associated but disarticulated, as in the case of the *Halisaurus* and the turtle.

Many of these bones also show crushing and breakage. Some damage may reflect post-mortem damage to the bones, which is common in Couche III. However, in such cases the various pieces should be found in close association. In the case of the *Gavialomimus* rostrum (SI Fig. 2), the posterior ends of the maxillae are simply absent; this implies that these remains were broken apart before they fell to the seabed.

The patterns of damage seen here resemble those of fossils interpreted as having been digested by predators. Lizard and mammal jaws are sometimes found with enamel and dentine dissolved away, and have been interpreted as being eaten by predators such as carnivorous mammals, predatory birds, or crocodilians. Experimental studies of *Alligator* show stomach acids attack the enamel, and dentine of the tooth crowns before bones (Fisher, 1981). Similarly, studies of jaws eaten by mammalian carnivores show that stomach acids attack enamel first (Andrews and Evans, 1983). Bones may be protected from acids by skin and muscle in the initial phases of digestion; the collagen matrix of bones may also protect them from digestion because to a degree. But bones can still be damaged by stomach acids, as seen in the elasmosaurid (Fig. 19) and *Eremiasaurus* (SI Fig. 1). Here, bone damage resembles that of plesiosaur bone found inside a *Tylosaurus* skeleton (Everhart, 2004).

Such large fossils could not have passed through a mosasaur's gut. Instead they may have been egested as gastric pellets (Myhrvold, 2012). Gastric pellets are made by a wide range of species, including birds, mammals, and reptiles; notably, varanid lizards and carnivorous snakes (Myhrvold, 2012). As squamates, Mosasaurids presumably were broadly similar to snakes and lizards in their digestive systems, including the ability to produce gastric pellets. Many aquatic and piscivorous animals also produce gastric pellets, including sperm whales, pinnipeds, alligators, crocodiles, gulls, terns, albatross, cormorants, and kingfishers (Myhrvold, 2012).

By analogy, we suggest that the fossils found here represent animals or parts of animals ingested by mosasaurids, digested by stomach acid, and vomited up. In some specimens, such as the *Halisaurus* and elasmosaurid skulls (Fig. 19 and SI Figs. 3–5), bone association is retained, and with the turtle and fish, two different species are associated (Fig. 19 and SI Fig. 6). In other cases, the

UNCORRECTED PROOF

gastric pellets appear to be poorly consolidated and so the remains are isolated.

In the absence of direct association in the form of gut contents, we cannot reject the possibility that other large mosasaurids such as *Mosasaurus* or *Eremiasaurus* preyed on smaller ones. However, the most likely predator is *Thalassotitan*, given its abundance in the assemblage, and given that no other mosasaurid has the combination of large size, massive jaws and teeth, and tooth wear seen in *Thalassotitan*.

Mosasaurus beaugei grew to large size (Bardet et al., 2004), but its more gracile skull, and slender jaws and teeth instead suggest a diet of large fish (Bardet et al., 2015). Gut contents of *Mosasaurus* also suggest piscivorous habits (Konishi et al., 2014). *Mosasaurus* seems unlikely to have routinely consumed large marine reptiles, but some of the fish remains found here could conceivably have been eaten by it. *Eremiasaurus* has large, bladelike lateral teeth and shows limited tooth wear (LeBlanc et al., 2012; Bardet et al., 2015). It might have preyed on marine reptiles, but as did not grow to large size, and so is unlikely to have eaten large ones.

The possibility that these remains result from predation or scavenging by sharks also seems unlikely. Sharks typically feed by stripping meat off bones, gripping the food and sawing back and forth with the jaws. This leaves distinctive toothmarks (Allaire et al., 2012) and bones recovered from shark stomachs are covered with such toothmarks where the sharks attempted to deflesh bones before swallowing them (Işcan and McCabe, 1995). These traces are known from marine reptile bones, including mosasaurids (Bardet et al., 1998; Corral et al., 2004); for instance, MNHM.KH.231 shows shark bites on its surangular (Fig. 4). None of the digested bones examined here show traces of shark feeding, however. There is also little muscle on mosasaurid mandibles, so sharks seem unlikely to target them. Instead, consumption of jaws and skulls suggests these animals were either swallowed whole-as snakes do, and as varanids do with small prey- or torn apart and the pieces swallowed, as in crocodilians.

Pathology

Thalassotitan appears to have lived a violent life. Healing lesions are seen in a large proportion of individuals described here. MHNM KH.324 exhibits two small, crater-like lesions on the left maxilla (Fig. 10). MHNM KH.326, a large dentary, shows irregular bone on the ventrolateral aspect of the jaw tip (Fig. 12C). MHNM.KH.396 also shows pathological bone on the right maxilla (Fig. 13C, D). MHNM.KH.325 shows large, crater-like depressions on the dentary's ventrolateral surface (Fig. 14C) and a small bony spur on its lateral surface (Fig. 14D). A large dentary (Fig. 14) shows a large, elliptical, crater-like lesion near the tip of the left lower jaw, and several small lumps of bone on the jaw's lateral surface. Highly irregular woven bone texture on the maxilla of another specimen (Fig. 13C, D) suggests injury in the late stages of healing.

These injuries resemble those attributed to face-biting in mosasaurids (Everhart, 2008) and other lepidosaurs (Evans, 1983). Similar injuries occur on the jaws of crocodiles and dinosaurs, including tyrannosaurids (Tanke and Currie, 1998; Peterson et al., 2009; Brown et al., 2021). Bite marks on the jaws and face are common in mosasaurids, occurring in *Mosasaurus hoffmanni* (Lingham-Soliar, 2004; Street and Caldwell, 2017), *Prognathodon currii* (Christiansen and Bonde, 2002), *Prognathodon* cf. *sectorius* (Bastiaans et al., 2020), *Clidastes propython* (Everhart, 2008), *Platecarpus* (Lingham-Soliar, 2004), *Tylosaurus nepaeolicus*, *T. kansasensis* (Everhart, 2008) and *Pluridens serpentis* (Longrich et al., 2021a). However, such bite traces are exceptionally frequent in *Thalassotitan*. Almost half the specimens described here show trauma. This likely underestimates the actual per-individual injury rate, since not every bone in every specimen can be examined. Such injuries suggest frequent, violent confrontations with other marine reptiles, most likely with other members of the species. Fights may have taken place over feeding grounds, access to mates, or both.

6. *Thalassotitan* compared to modern marine apex predators

Evidence from anatomy, tooth wear, and the fossil assemblage suggests that *Thalassotitan* was a specialized apex predator. Its lifestyle likely resembled that of modern orcas, white sharks, and the extinct sperm whale *Livyatan*. Orcas, which resemble *Thalassotitan* in terms of their teeth and jaws, may provide an analogy for the paleobiology of *Thalassotitan*. Orcas have varied feeding strategies. Some prey extensively on other marine mammals (Jefferson et al., 1991). These include seals, sea lions, sea otter, dugong, dolphins, porpoises, beaked whales, even large baleen and sperm whales. Orcas sometimes take sea turtles (Pitman and Dutton, 2004), and scavenge on baleen whales (Whitehead and Reeves, 2005). Other specialize on fish (Jefferson et al., 1991), or sharks (Ford et al., 2011). However, as discussed above, *Thalassotitan* resembles marine-mammal specialist orcas in terms of its teeth, suggesting it preyed on marine tetrapods.

Great white sharks differ in their tooth morphology, but have a similar feeding strategy. Great whites feed on marine mammals such as seals and sea lions, small cetaceans including dolphins, porpoises, and beaked whales; rarely they attack large whales such as humpback. Great whites also eat sea turtles, large fish like tuna and swordfish, and sometimes other sharks (Long and Jones, 1996; Boldrocchi et al., 2017) (Dines and Gennari, 2020). Great Whites also scavenge whale carcasses (Long and Jones, 1996). Juveniles, however, primarily eat fish (Estrada et al., 2006) (Boldrocchi et al., 2017).

In light of the paleobiological evidence discussed above, we suggest *Thalassotitan* resembled transient orcas and white sharks in feeding habits, preying on marine tetrapods, large fish, and sharks. Potential prey in the phosphates included a dozen species of mosasaurids, sea turtles, elasmosaurids, large fish such as *Enchodus*, and a plethora of sharks. All were likely prey; *Thalassotitan* may also have scavenged when possible.

Similar to modern apex predators like orcas and white sharks, *Thalassotitan* and other giant prognathodontins such as *Prognathodon saturator* appear to have been widespread. *Thalassotitan* and its relatives are currently known from the Maastrichtian of Africa, Europe, the Middle East, and South America (Fig. 20). So far, however, they remain unknown from Maastrichtian assemblages in New Jersey, California, Chile, Japan, or New Zealand.

7. Implications for K–Pg extinction

Thalassotitan was the top predator in the Moroccan marine fauna, but only part of a diverse mosasaur fauna existing in the latest Cretaceous. Maastrichtian mosasaurs were characterized by a remarkable diversity of jaw and tooth shapes, including piercing, cutting, and crushing teeth (Bardet et al., 2015; Strong et al., 2020; Longrich et al., 2021b); these tooth morphologies imply a wide range of prey. Small mosasaurs likely took small prey like cephalopods, small fish, hard-shelled prey like bivalves, sea urchins, crustaceans, and ammonites. Larger mosasaurs likely took large fish and, in the case of *Thalassotitan*, other marine reptiles. The high variability in stable isotopes in mosasaur teeth supports the idea

UNCORRECTED PROOF

that different taxa exploited different food (Schulp et al., 2013b). Mosasaurs also showed a remarkable range in body size, from the small *Xenodens* and *Halisaurus* to the giant *Mosasaurus* and *Prognathodon*. Mosasaurs also vary in how they exploited the ocean depths; some were deep divers, others were surface feeders (Rothschild and Martin, 2005). And they show habitat specialization; giant prognathodontins for example so far are known only from the eastern Atlantic of Europe and Africa, and the Tethys of North Africa and the Middle East.

Mosasaurids comprised a fraction of total diversity and biomass in Late Cretaceous seas. Yet as predators, they sat atop of the marine food chain, and so offer insights into ecosystem evolution. Diversity and abundance of predators reflects the structure of marine ecosystems. Marine productivity exerts a bottom-up effect on predators; high productivity and prey abundance at lower trophic levels can increase predator abundance (Frederiksen et al., 2006); species richness of prey also drives predator species richness (Sandom et al., 2013). The diversity and specialization of Moroccan mosasaurs therefore suggest high diversity of prey species; the existence of giant predators like *Thalassotitan* implies high prey abundance and productivity.

Marine predator diversity can therefore serve as a proxy for the diversity and complexity of marine ecosystems. If so, mosasaurid diversity – characterized by high species richness, high functional diversity, and high endemism (Longrich et al., 2021a; Longrich et al., 2021b) - suggest diverse, complex marine ecosystems existed before the K–Pg extinction. The appearance of giant apex predators, and the overall diversity of Maastrichtian mosasaurids, argue against ecosystem decline prior to the K–Pg extinction. Instead, these patterns suggest increasing diversification and specialization in marine faunas (Bardet et al., 2015; Bardet et al., 2017).

8. Conclusions

A new mosasaurid, *Thalassotitan atrox*, is described on the basis of fossils from the upper Maastrichtian phosphates of Morocco. This new mosasaurid is characterized by its large size, robust jaws and teeth, and adaptations for high bite force. A number of lines of evidence, including the structure of the jaws and teeth, tooth wear, and associated fossils suggest it acted as an apex predator, similar to killer whales and white sharks. It was part of a diverse marine vertebrate fauna that existed just prior to the K–Pg extinction.

Declaration of competing interest

The authors declare that they have no known competing financial interests or personal relationships that could have appeared to influence the work reported in this paper.

Acknowledgments

Thanks to Mustapha Meharich for assistance in Morocco, and to all OCP staff for logistical support during fieldwork and help in preparing the specimens under their care. Thanks also to the CR2P (MNHN, Paris) technical staff for their help and work both during fieldwork and at the laboratory, namely Jean-Michel Pacaud and Batz le Dimet for preparation of specimens, to Denis Serrette and Philippe Loubry for the photographs and to Alexandre Lethiers for the interpretative drawings. Thanks to Jacques Gauthier and Mike Everhart for discussions, and to Johann Lindgren for informations on mosasaurids. Finally, thanks to Jahn Hornung, Eric Mulder, and László Makádi, whose constructive criticism has greatly improved this paper.

References

Allaire, M.T., Manhein, M.H., Burgess, G.H., 2012. Shark-Inflicted Trauma: a case study of unidentified remains recovered from the Gulf of Mexico. Journal of Forensic Sciences 57, 1675–1678.

Alvarez, L.W., Alvarez, W., Asaro, F., Michel, H.V., 1980. Extraterrestrial cause for the Cretaceous-Tertiary extinction. Science 208, 1095–1108.

Álvarez-Herrera, G., Agnolin, F., Novas, F., 2020. A rostral neurovascular system in the mosasaur *Taniwhasaurus antarcticus*. The Science of Nature 107, 1–5.

Andrews, P., Evans, E.N., 1983. Small mammal bone accumulations produced by mammalian carnivores. Paleobiology 289–307.

Arambourg, C., 1952. Les vertébrés fossiles des gisements de phosphates (Maroc-Algérie-Tunisie). Notes et Mémoires du Service Géologique du Maroc 92, 1–372.

Archibald, J.D., Bryant, L.J., 1990. Differential Cretaceous–Tertiary extinction of nonmarine vertebrates; evidence from northeastern Montana. In: Sharpton, V.L., Ward, P.D. (Eds.), Global Catastrophes in Earth History: an Interdisciplinary Conference on Impacts, Volcanism, and Mass Mortality: Geological Society of America Special Paper, Vol. 247, pp. 549–562.

Archibald, J.D., Clemens, W., Padian, K., Rowe, T., Macleod, N., Barrett, P.M., Gale, A., Holroyd, P., Sues, H.-D., Arens, N.C., 2010. Cretaceous extinctions: multiple causes. Science 328, 973 author reply 975.

Arnold, E., 1988. Cranial Kinesis in Lizards, Evolutionary Biology. Springer, pp. 323–357.

Bardet, N., 2012. Maastrichtian marine reptiles of the Mediterranean Tethys: a palaeobiogeographical approach. Bulletin de la Societe Geologique de France 183, 573–596.

Bardet, N., Pereda-Suberbiola, X., 2002. Marine reptiles from the Late Cretaceous Phosphates of Jordan: palaeobiogeographical implications. Geodiversitas 24, 831–839.

Bardet, N., Jagt, J., Kuypers, M., Dortangs, R., 1998. Shark tooth marks on a vertebra of the mosasaur *Plioplatecarpus marshi* from the Late Maastrichtian of Belgium. Publicaties van het Natuurhistorisch Genootschap in Limburg 41, 52–55.

Bardet, N., Pereda-Suberbiola, X., Jalil, N.-E., 2003. A new mosasauroid (Squamata) from the Late Cretaceous (Turonian) of Morocco. Comptes Rendus Palevol 2, 607–616.

Bardet, N., Pereda-Suberbiola, X., Iarochène, M., Bouyahyaoui, F., Bouya, B., Amaghzaz, M., 2004. *Mosasaurus beaugei* Arambourg, 1952 (Squamata, Mosasauridae) from the Late Cretaceous phosphates of Morocco. Geobios 37, 315–324.

Bardet, N., Pereda-Suberbiola, X., Iarochène, M., Amalik, M., Bouya, B., 2005a. Durophagous Mosasauridae (Squamata) from the Upper Cretaceous phosphates of Morocco, with description of a new species of *Globidens*. Netherlands Journal of Geosciences 84, 167–175.

Bardet, N., Pereda-Suberbiola, X., Iarochène, M., Bouya, B., Amaghzaz, M., 2005b. A new species of *Halisaurus* from the Late Cretaceous phosphates of Morocco, and the phylogenetical relationships of the Halisaurinae (Squamata: Mosasauridae). Zoological Journal of the Linnean Society 143, 447–472.

Bardet, N., Pereda-Suberbiola, X., Schulp, A.S., Bouya, B., 2008. New material of *Carinodens* (Squamata, Mosasauridae) from the Maastrichtian (Late Cretaceous) phosphates of Morocco. In: Proceedings of the Second Mosasaur Meeting. Fort Hays Studies, Special, pp. 29–36.

Bardet, N., Pereda-Suberbiola, X., Jouve, S., Bourdon, E., Vincent, P., Houssaye, A., Rage, J.-C., Jalil, N.-E., Bouya, B., Amaghzaz, M., 2010. Reptilian assemblages from the latest Cretaceous–Palaeogene phosphates of Morocco: from Arambourg to present time. Historical Biology 22, 186–199.

Bardet, N., Jalil, N.-E., de Lapparent de Broin, F., Germain, D., Lambert, O., Amaghzaz, M., 2013. A Giant Chelonioid Turtle from the Late Cretaceous of Morocco with a Suction Feeding Apparatus Unique among Tetrapods. PLoS One 8, e63586.

Bardet, N., Houssaye, A., Vincent, P., Pereda-Suberbiola, X., Amaghzaz, M., Jourani, E., Meslouh, S., 2015. Mosasaurids (Squamata) from the Maastrichtian phosphates of Morocco: biodiversity, palaeobiogeography and palaeoecology based on tooth morphoguilds. Gondwana Research 27, 1068–1078.

Bardet, N., Gheerbrant, E., Noubhani, A., Cappetta, H., Jouve, S., Bourdon, E., Pereda-Suberbiola, X., Jalil, N.-E., Vincent, P., Houssaye, A., Solé, F., El Houssaini Darif, K., Adnet, S., Rage, J.-C., Lapparent de Broin de, F., Sudre, J., Bouya, B., Amaghzaz, M., Meslouh, S., 2017. Mémoires de la Société Géologique de France N.S.. Les Vertébrés des Phosphates Crétacés-paléogènes (72, 1-47, 8 Ma) du Maroc, vol. 180, pp. 351–452.

Bastiaans, D., Kroll, J.J., Cornelissen, D., Jagt, J.W., Schulp, A.S., 2020. Cranial palaeopathologies in a Late Cretaceous mosasaur from the Netherlands. Cretaceous Research 112, 104425.

Bell Jr., G.L., 1997. A phylogenetic revision of North American and Adriatic Mosasauroidea, Ancient marine reptiles. Elsevier, pp. 293–332.

Bernard, A., Lécuyer, C., Vincent, P., Amiot, R., Bardet, N., Buffetaut, E., Cuny, G., Fourel, F., Martineau, F., Mazin, J.-M., 2010. Regulation of body temperature by some Mesozoic marine reptiles. Science 328, 1379–1382.

UNCORRECTED PROOF

Boldrocchi, G., Kiszka, J., Purkis, S., Storai, T., Zinzula, L., Burkholder, D., 2017. Distribution, ecology, and status of the white shark, *Carcharodon carcharias*, in the Mediterranean Sea. Reviews in Fish Biology and Fisheries 27, 515–534.

Bonde, N., Christiansen, P., 2003. New dinosaurs from Denmark. Comptes Rendus Palevol 2, 13–26.

Brochu, C.A., 2002. Osteology of *Tyrannosaurus rex*: insights from a nearly complete skeleton and high-resolution computed tomographic analysis of the skull. Journal of Vertebrate Paleontology, Memoirs 7, 1–138.

Brown, C.M., Currie, P.J., Therrien, F., 2021. Intraspecific facial bite marks in tyrannosaurids provide insight into sexual maturity and evolution of bird-like intersexual display. Paleobiology 1–32.

Cappetta, H., 1987. Chondrichthyes II. Mesozoic and Cenozoic Elasmobranchii. Handbook of paleoichthyology 3, 1–193.

Cappetta, H., Bardet, N., Pereda-Suberbiola, X., Adnet, S., Akkrim, D., Amalik, M., Benabdallah, A., 2014. Marine vertebrate faunas from the Maastrichtian phosphates of Benguérir (Ganntour Basin, Morocco): Biostratigraphy, palaeobiogeography and palaeoecology. Palaeogeography, Palaeoclimatology, Palaeoecology 409, 217–238.

Christiansen, P., Bonde, N., 2002. A new species of gigantic mosasaur from the Late Cretaceous of Israel. Journal of Vertebrate Paleontology 22, 629–644.

Cooper, S.L., Marson, K.J., Smith, R.E., Martill, D., 2021. Contrasting preservation in pycnodont fishes reveals first record of regurgitalites from the Upper Cretaceous (Maastrichtian) Moroccan phosphate deposits. Cretaceous Research, 105111.

Corral, J.C., Suberbiola, X.P., Bardet, N., 2004. Marcas de ataque atribuidas a un seláceo en una vértebra de mosasaurio del Cretácico Superior de Álava (región Vasco-Cantábrica). Spanish Journal of Palaeontology 19, 23–32.

Cost, I.N., Middleton, K.M., Sellers, K.C., Echols, M.S., Witmer, L.M., Davis, J.L., Holliday, C.M., 2020. Palatal biomechanics and its significance for cranial kinesis in *Tyrannosaurus rex*. The Anatomical Record 303, 999–1017.

Dines, S., Gennari, E., 2020. First observations of white sharks (*Carcharodon carcharias*) attacking a live humpback whale (*Megaptera novaeangliae*). Marine and Freshwater Research 71, 1205–1210.

Dollo, L., 1889. Note sur les vertébrés récemment offerts au Musée de Bruxelles par M. Alfred Lemonniet. Bulletin de la Societe Belge de Geologie de Paleontologie et d'Hydrologie 3, 181–182.

Dollo, L., 1904. Les Mosasauriens de la Belgique. Bulletin de la Société Belge de Géologie, de Paléontologie et Hydrologie, pp. 207–216.

Dortangs, R.W., Schulp, A.S., Mulder, E.W.A., Jagt, J.W.M., Peeters, H.H.G., Graaf, D.T.d., 2002. A large new mosasaur from the Upper Cretaceous of The Netherlands. Netherlands Journal of Geosciences 81, 1–8.

Erickson, G.M., Van Kirk, S.D., Su, J., Levenston, M.E., Caler, W.E., Carter, D.R., 1996. Bite-force estimation for *Tyrannosaurus rex* from tooth-marked bones. Nature 382, 706–708.

Estrada, J.A., Rice, A.N., Natanson, L.J., Skomal, G.B., 2006. Use of isotopic analysis of vertebrae in reconstructing ontogenetic feeding ecology in white sharks. Ecology 87, 829–834.

Evans, S.E., 1983. Mandibular fracture and inferred behavior in a fossil reptile. Copeia 1983, 845–847.

Everhart, M.J., 2004. Plesiosaurs as the Food of Mosasaurs; New Data on the Stomach contents of *Tylosaurus proriger* (Squamata; Mosasauridae) from the Niobrara Formation of Western Kansas. The Mosasaur 7, 41–46.

Everhart, M.J., 2008. A bitten skull of *Tylosaurus kansasensis* (Squamata: Mosasauridae) and a review of mosasaur-on-mosasaur pathology in the fossil record. Transactions of the Kansas Academy of Science 111, 251–262.

Farlow, J.O., Brinkman, D.L., 1994. Wear surfaces on the teeth of tyrannosaurs, Vol. 7. The Paleontological Society Special Publications, pp. 165–176.

Fastovsky, D.E., Sheehan, P.M., 2005. The extinction of the dinosaurs in North America. Geological Society of America Today 15, 4–10.

Fisher, D.C., 1981. Crocodilian scatology, microvertebrate concentrations, and enamel-less teeth. Paleobiology 262–275.

Ford, J.K., Ellis, G.M., Matkin, C.O., Wetklo, M.H., Barrett-Lennard, L.G., Withler, R.E., 2011. Shark predation and tooth wear in a population of northeastern Pacific killer whales. Aquatic Biology 11, 213–224.

Frazzetta, T., 1962. A functional consideration of cranial kinesis in lizards. Journal of Morphology 111, 287–319.

Frederiksen, M., Edwards, M., Richardson, A.J., Halliday, N.C., Wanless, S., 2006. From plankton to top predators: bottom-up control of a marine food web across four trophic levels. Journal of Animal Ecology 75, 1259–1268.

Frey, E., Tarsitano, S., Oelofsen, B., Riess, J., 2001. The origin of temporal fenestrae. South African Journal of Science 97, 334–336.

Gauthier, J., Kearney, M., Maisano, J.A., Rieppel, O., Behlke, A., 2012. Assembling the squamate tree of life: perspectives from the phenotype and the fossil record. Bulletin Yale Peabody Museum 53, 3–308.

Gemmellaro, M., 1921. Rettili Maëstrichtiani di Egitto. Arti graf. G. Castiglia.

Gervais, P., 1852. Zoologie et Paléontologie Françaises (Animaux Vertébrés): Nouvelles Recherches sur les Animaux Vivants del la France. Arthus Bertrand, Paris.

Gignac, P.M., Erickson, G.M., 2017. The biomechanics behind extreme osteophagy in *Tyrannosaurus rex*. Scientific Reports 7, 1–10.

Gilmore, C.W., 1912. A new mosasauroid reptile from the Cretaceous of Alabama. Proceedings of the United States National Museum 41, 479–484.

Gordon, J.E., 1978. Structures: Or, Why Things Don't Fall Down. Plenum, New York.

Grigoriev, D., 2013. Redescription of *Prognathodon lutugini* (Squamata, Mosasauridae). Труды Зоологического института РАН 317, 246–261.

Herrel, A., De Vree, F., Delheusy, V., Gans, C., 1999. Cranial kinesis in gekkonid lizards. Journal of Experimental Biology 202, 3687–3698.

Ikejiri, T., Lucas, S., 2015. Osteology and taxonomy of *Mosasaurus conodon* Cope 1881 from the Late Cretaceous of North America. Netherlands Journal of Geosciences 94, 39–54.

Işcan, M.Y., McCabe, B.Q., 1995. Analysis of human remains recovered from a shark. Forensic Science International 72, 15–23.

Jefferson, T.A., Stacey, P.J., Baird, R.W., 1991. A review of killer whale interactions with other marine mammals: predation to co-existence. Mammal Review 21, 151–180.

Jouve, S., Bardet, N., Jalil, N.-E., Pereda-Suberbiola, X., Bouya, B., Amaghzaz, M., 2008. The oldest African crocodylian: phylogeny, paleobiogeography, and differential survivorship of marine reptiles through the Cretaceous-Tertiary boundary. Journal of Vertebrate Paleontology 28, 409–421.

Kaddumi, H.F., 2009. The First and Most Complete *Carinodens* (Squamata: Mosasauridae) Skeleton Yet with a Description of a New Species from the Harrana Fauna, Fossils of the Harrana Fauna and the Adjacent Areas. Publications of the Eternal River Museum of Natural History Amman, pp. 49–64.

Kocsis, L., Gheerbrant, E., Mouflih, M., Cappetta, H., Yans, J., Amaghzaz, M., 2014. Comprehensive stable isotope investigation of marine biogenic apatite from the Late Cretaceous–Early Eocene phosphate series of Morocco. Palaeogeography, Palaeoclimatology, Palaeoecology 394, 74–88.

Konishi, T., Brinkman, D., Massare, J.A., Caldwell, M.W., 2011. New exceptional specimens of *Prognathodon overtoni* (Squamata, Mosasauridae) from the upper Campanian of Alberta, Canada, and the systematics and ecology of the genus. Journal of Vertebrate Paleontology 31, 1026–1046.

Konishi, T., Lindgren, J., Caldwell, M.W., Chiappe, L., 2012. *Platecarpus tympaniticus* (Squamata, Mosasauridae): osteology of an exceptionally preserved specimen and its insights into the acquisition of a streamlined body shape in mosasaurs. Journal of Vertebrate Paleontology 32, 1313–1327.

Konishi, T., Newbrey, M.G., Caldwell, M.W., 2014. A small, exquisitely preserved specimen of *Mosasaurus missouriensis* (Squamata, Mosasauridae) from the upper Campanian of the Bearpaw Formation, western Canada, and the first stomach contents for the genus. Journal of Vertebrate Paleontology 34, 802–819.

Lambert, O., Bianucci, G., Post, K., De Muizon, C., Salas-Gismondi, R., Urbina, M., Reumer, J., 2010. The giant bite of a new raptorial sperm whale from the Miocene epoch of Peru. Nature 466, 105–108.

Lapparent de Broin, F.d., Bardet, N., Amaghzaz, M., Meslouh, S., 2013. A strange new chelonioid turtle from the Latest Cretaceous phosphates of Morocco. Comptes Rendus Palevol 13, 87–95.

LeBlanc, A.R.H., Caldwell, M.W., Bardet, N., 2012. A new mosasaurine from the Maastrichtian (Upper Cretaceous) phosphates of Morocco and its implications for mosasaurine systematics. Journal of Vertebrate Paleontology 32, 82–104.

LeBlanc, A.R., Caldwell, M.W., Lindgren, J., 2013. Aquatic adaptation, cranial kinesis, and the skull of the mosasaurine mosasaur *Plotosaurus bennisoni*. Journal of Vertebrate Paleontology 33, 349–362.

Lindgren, J., Siverson, M., 2004. The first record of the mosasaur *Clidastes* from Europe and its palaeogeographical implications. Acta Palaeontologica Polonica 49.

Lindgren, J., Caldwell, M.W., Jagt, J.W., 2008. New data on the postcranial anatomy of the California mosasaur *Plotosaurus bennisoni* (Camp, 1942) (Upper Cretaceous: Maastrichtian), and the taxonomic status of *P. tuckeri* (Camp, 1942). Journal of Vertebrate Paleontology 28, 1043–1054.

Lingham-Soliar, T., Nolf, D., 1989. The mosasaur *Prognathodon* (Reptilia, Mosasauridae) from the Upper Cretaceous of Belgium. Bulletin de l'Institut Royal des Sciences Naturelles de Belgique, Sciences de la Terre 59, 137–190.

Lingham-Soliar, T., 1995. Anatomy and functional morphology of the largest marine reptile known, *Mosasaurus hoffmanni* (Mosasauridae, Reptilia) from the Upper Cretaceous, Upper Maastrichtian of the Netherlands. Philosophical Transactions of the Royal Society of London. Series B: Biological Sciences 347, 155–180.

Lingham-Soliar, T., 1999. The Durophagous Mosasaurs (Lepidosauromorpha, Squamata) Globidens and Carinodens from the Upper Cretaceous of Belgium and The Netherlands. Палеонтологический Журнал 41–43.

Lingham-Soliar, T., 2004. Palaeopathology and injury in the extinct mosasaurs (Lepidosauromorpha, Squamata) and implications for modern reptiles. Lethaia 37, 255–262.

Lively, J.R., 2018. Taxonomy and historical inertia: *Clidastes* (Squamata: Mosasauridae) as a case study of problematic paleobiological taxonomy. Alcheringa: An Australasian Journal of Palaeontology 42, 516–527.

Lively, J.R., 2020. Redescription and phylogenetic assessment of '*Prognathodon*' *stadtmani*: implications for Globidensini monophyly and character homology in Mosasaurinae. Journal of Vertebrate Paleontology 40, e1784183.

Long, D.J., Jones, R.E., 1996. White shark predation and scavenging on cetaceans in the eastern North Pacific Ocean. In: Great white sharks: the biology of *Carcharodon carcharias*, pp. 293–307.

Longrich, N.R., Horner, J.R., Erickson, G.M., Currie, P.J., 2010. Cannibalism in *Tyrannosaurus rex*. PLoS One 5 (10), e13419, 13410.11371/journal.pone.0013419.

Longrich, N.R., Tokaryk, T.T., Field, D., 2011. Mass extinction of birds at the Cretaceous-Paleogene (K-Pg) boundary. Proceedings of the National Academy of Sciences 108, 15253–15257.

Longrich, N.R., Bhullar, B.-A.S., Gauthier, J., 2012. Mass extinction of lizards and snakes at the Cretaceous-Paleogene boundary. Proceedings of the National Academy of Sciences 109, 21396–21401.

UNCORRECTED PROOF

Longrich, N.R., Scriberas, J., Wills, M.A., 2016. Severe extinction and rapid recovery of mammals across the Cretaceous-Paleogene boundary, and the effects of rarity on patterns of extinction and recovery. Journal of Evolutionary Biology. https://doi.org/10.1111/jeb.12882.

Longrich, N.R., Pereda-Suberbiola, X., Jalil, N.-E., Khaldoune, F., Jourani, E., 2017. An abelisaurid from the latest Cretaceous (late Maastrichtian) of Morocco, North Africa. Cretaceous Research 76, 40–52.

Longrich, N.R., Martill, D.M., Andres, B., 2018. Late Maastrichtian pterosaurs from North Africa and mass extinction of Pterosauria at the Cretaceous-Paleogene boundary. PLoS Biology 16, e2001663.

Longrich, N.R., Bardet, N., Khaldoune, F., Yazami, O.K., Jalil, N.-E., 2021a. *Pluridens serpentis*, a new mosasaurid (Mosasauridae: Halisaurinae) from the Maastrichtian of Morocco and implications for mosasaur diversity. Cretaceous Research, 104882.

Longrich, N.R., Bardet, N., Schulp, A.S., Jalil, N.-E., 2021b. *Xenodens calminechari* gen. et sp. nov., a bizarre mosasaurid (Mosasauridae, Squamata) with shark-like cutting teeth from the upper Maastrichtian of Morocco, North Africa. Cretaceous Research, 104764.

Longrich, N.R., Pereda-Suberbiola, X., Pyron, R.A., Jalil, N.-E., 2021c. The first duckbill dinosaur (Hadrosauridae: Lambeosaurinae) from Africa and the role of oceanic dispersal in dinosaur biogeography. Cretaceous Research 120, 104678.

Luan, X., Walker, C., Dangaria, S., Ito, Y., Druzinsky, R., Jarosius, K., Lesot, H., Rieppel, O., 2009. The mosasaur tooth attachment apparatus as paradigm for the evolution of the gnathostome periodontium. Evolution and Development 11, 247–259.

Machalski, M., Jagt, J.W., Dortangs, R.W., Mulder, E.W., Radwanski, A., 2003. Campanian and Maastrichtian mosasaurid reptiles from central Poland. Acta Palaeontologica Polonica 48, 397–408.

Martin, J.E., 2007. A new species of the durophagous mosasaur, *Globidens* (Squamata: Mosasauridae) from the Late Cretaceous Pierre Shale Group of central South Dakota, USA, Vol. 427. Special Papers-Geological Society of America, p. 177.

Martin, J.E., Vincent, P., Tacail, T., Khaldoune, F., Jourani, E., Bardet, N., Balter, V., 2017. Calcium isotopic evidence for vulnerable marine ecosystem structure prior to the K/Pg extinction. Current Biology 27, 1641–1644 e1642.

McCurry, M.R., Evans, A.R., Fitzgerald, E.M., Adams, J.W., Clausen, P.D., McHenry, C.R., 2017a. The remarkable convergence of skull shape in crocodilians and toothed whales. Proceedings of the Royal Society B: Biological Sciences 284, 20162348.

McCurry, M.R., Fitzgerald, E.M., Evans, A.R., Adams, J.W., McHenry, C.R., 2017b. Skull shape reflects prey size niche in toothed whales. Biological Journal of the Linnean Society 121, 936–946.

Myhrvold, N.P., 2012. A call to search for fossilised gastric pellets. Historical Biology 24, 505–517.

Oppel, M., 1811. Die Ordnungen, Familien und Gattungen der Reptilien als Prodrom einer Naturgeschichte derselben. Lindauer, München.

Owen, R., 1846. A history of British fossil mammals, and birds. J. Van Voorst.

Páramo-Fonseca, M.E., 2013. *Eonatator coellensis* nov. sp.(Squamata: Mosasauridae), a new species from the Upper Cretaceous of Colombia. Revista de la Academia Colombiana de Ciencias Exactas, Físicas y Naturales 37, 499–518.

Pereda-Suberbiola, X., Bardet, N., Jouve, S., Iarochène, M., Bouya, B., Amaghzaz, M., 2003. A new azhdarchid pterosaur from the Late Cretaceous phosphates of Morocco. Geological Society, London, Special Publications 217, 79–90.

Pereda-Suberbiola, X., Bardet, N., Iarochène, M., Bouya, B., Amaghzaz, M., 2004. The first record of a sauropod dinosaur from the Late Cretaceous phosphates of Morocco. Journal of African Earth Sciences 40, 81–88.

Peterson, J.E., Henderson, M.D., Scherer, R.P., Vittore, C.P., 2009. Face biting on a juvenile tyrannosaurid and behavioral implications. PALAIOS 24, 780–784.

Pitman, R.L., Dutton, P.H., 2004. Killer whale predation on a leatherback turtle in the northeast Pacific. Pacific Science 58, 497–498.

Polcyn, M.J., Lindgren, J., Bardet, N., Cornelissen, D., Verding, L., Schulp, A.S., 2012. Description of new specimens of *Halisaurus arambourgi* Bardet & Pereda Suberbiola, 2005 and the relationships of Halisaurinae. Bulletin de la Societe Geologique de France 183, 123–136.

Price, L.I., 1957. A presença de *Globidens* no Cretácico superior do Brasil. Divisão de Geologia e Mineralogia, Boletim 169, 1–24.

Raab, M., 1963. Fossil fish and reptiles from Late Campanian phosphatic deposits of the Negev Region of Israel.

Rieppel, O., Kearney, M., 2005. Tooth replacement in the Late Cretaceous mosasaur *Clidastes*. Journal of Herpetology 39, 688–692.

Rothschild, B., Martin, L., 2005. Mosasaur ascending: the phylogeny of bends. Netherlands Journal of Geosciences 84, 341–344.

Russell, D.A., 1967. Systematics and morphology of American mosasaurs. Bulletin - Peabody Museum of Natural History 23, 1–240.

Russell, D.A., 1975. A new species of *Globidens* from South Dakota, and a review of globidentine mosasaurs. Fieldiana Geology 33, 235–256.

Sandom, C., Dalby, L., Fløjgaard, C., Kissling, W.D., Lenoir, J., Sandel, B., Trøjelsgaard, K., Ejrnæs, R., Svenning, J.-C., 2013. Mammal predator and prey species richness are strongly linked at macroscales. Ecology 94, 1112–1122.

Schubert, B.W., Ungar, P.S., 2005. Wear facets and enamel spalling in tyrannosaurid dinosaurs. Acta Palaeontologica Polonica 50, 93–99.

Schulp, A.S., 2006. A comparative description of Prognathodon saturator (Mosasauridae, Squamata), with notes on its phylogeny, Vol. 45. Publicaties van het Natuurhistorisch Genootschap in Limburg, pp. 19–56.

Schulp, A.S., Polcyn, M.J., Mateus, O., Jacobs, L.L., Morais, M.L., 2008. A new species of *Prognathodon* (Squamata, Mosasauridae) from the Maastrichtian of Angola, and the affinities of the mosasaur genus *Liodon*. In: Proceedings of the Second Mosasaur Meeting, Fort Hays Studies Special Issue, Vol. 3, pp. 1–12.

Schulp, A.S., Bardet, N., Bouya, B., 2009. A new species of the durophagous mosasaur *Carinodens* (Squamata, Mosasauridae) and additional material of *Carinodens belgicus* from the Maastrichtian phosphates of Morocco. Netherlands Journal of Geosciences 88, 161–167.

Schulp, A., Polcyn, M., Mateus, O., Jacobs, L., 2013a. Two rare mosasaurs from the Maastrichtian of Angola and the Netherlands. Netherlands Journal of Geosciences 92, 3–10.

Schulp, A., Vonhof, H., Van der Lubbe, J., Janssen, R., Van Baal, R., 2013b. On diving and diet: resource partitioning in type-Maastrichtian mosasaurs. Netherlands Journal of Geosciences 92, 165–170.

Schulte, P., Alegret, L., Arenillas, I., Arz, J.A., Barton, P.J., Bown, P.R., Bralower, T.J., Christeson, G.L., Claeys, P., Cockell, C.S., Collins, G.S., Deutsch, A., Goldin, T.J., Goto, K., Grajales-Nishimura, J.M., Grieve, R.A.F., Gulick, S.P.S., Johnson, K.R., Kiessling, W., Koeberl, C., Kring, D.A., MacLeod, K.G., Matsui, T., Melosh, J., Montanari, A., Morgan, J.V., Neal, C.R., Nicholas, D.J., Norris, R.D., Pierazzo, E., Ravizza, G., Vieyra, R., Reimold, W.U., Robin, E., Salge, T., Speijer, R.P., Sweet, A.R., Urrutia-Fucugauchi, J., Vajda, V., Whalen, M.T., Willumsen, P.S., 2010. The Chicxulub Asteroid Impact and Mass Extinction at the Cretaceous-Paleogene Boundary. Science 327, 1214–1218.

Sereno, P.C., 1998. A rationale for phylogenetic definitions, with application to the higher-level taxonomy of Dinosauria. Neues Jahrbuch für Geologie und Paläontologie – Abhandlungen 210, 41–83.

Sheehan, P.M., Fastovsky, D.E., 1992. Major extinctions of land-dwelling vertebrates at the Cretaceous-Tertiary boundary, Eastern Montana. Geology 20, 556–560.

Sheehan, P.M., Fastovsky, D.E., Barreto, C., Hoffman, R.G., 2000. Dinosaur abundance was not declining in a "3m gap" at the top of the Hell Creek Formation, Montana and North Dakota. Geology 28, 523–526.

Simões, T.R., Vernygora, O., Paparella, I., Jimenez-Huidobro, P., Caldwell, M.W., 2017. Mosasauroid phylogeny under multiple phylogenetic methods provides new insights on the evolution of aquatic adaptations in the group. PLoS One 12, e0176773.

Smith, K.K., 1980. Mechanical significance of streptostyly in lizards. Nature 283, 778–779.

Snively, E., Henderson, D.M., Phillips, D.S., 2006. Fused and vaulted nasals of tyrannosaurid dinosaurs: implications for cranial strength and feeding mechanics. Acta Palaeontologica Polonica 51, 435–454.

Strand, E., 1926. Miscellanea nomenclatorica zoologica et palaeontologia. In: Archiv für Naturgeschichte Abt. A, Original-Arbeiten, Vol. 92, pp. 30–75.

Street, H.P., Caldwell, M.W., 2017. Rediagnosis and redescription of *Mosasaurus hoffmannii* (Squamata: Mosasauridae) and an assessment of species assigned to the genus *Mosasaurus*. Geological Magazine 154, 521–557.

Strong, C.R., Caldwell, M.W., Konishi, T., Palci, A., 2020. A new species of long-irostrine plioplatecarpine mosasaur (Squamata: Mosasauridae) from the Late Cretaceous of Morocco, with a re-evaluation of the problematic taxon '*Platecarpus*' *ptychodon*. Journal of Systematic Palaeontology 1–36.

Swofford, D.L., 2002, 4.0b10 ed.. PAUP*. Phylogenetic Analysis Using Parsimony (*and other methods). Sinauer Associates, Sunderland, Massachusetts.

Tanke, D.H., Currie, P.J., 1998. Head-biting behavior in the theropod dinosaurs: paleopathological evidence. Gaia 15, 167–184.

Van Valkenburgh, B., 1988. Incidence of tooth breakage among large, predatory mammals. The American Naturalist 131, 291–302.

Vincent, P., Bardet, N., Pereda Suberbiola, X., Bouya, B., Amaghzaz, M., Meslouh, S., 2011. *Zarafasaura oceanis*, a new elasmosaurid (Reptilia: Sauropterygia) from the Maastrichtian Phosphates of Morocco and the palaeobiogeography of latest Cretaceous plesiosaurs. Gondwana Research 19, 1062–1073.

Wainwright, P.C., Richard, B.A., 1995. Predicting patterns of prey use from morphology of fishes. Environmental Biology of Fishes 44, 97–113.

Whitehead, H., Reeves, R., 2005. Killer whales and whaling: the scavenging hypothesis. Biology Letters 1, 415–418.

Wiffen, J., 1990. New mosasaurs (Reptilia; Family Mosasauridae) from the Upper Cretaceous of North Island, New Zealand. New Zealand Journal of Geology and Geophysics 33, 67–85.

Williston, S.W., 1897. *Brachysaurus*, a new genus of mosasaurs, vol. 6. Kansas University Quarterly, pp. 95–98.

Yakovlev, N., 1901. Remains of the Late Cretaceous mosasaur from the south of Russia. Izvestiya Geologicheskogo Komiteta 20, 507–522.

Appendix A. Supplementary data

Supplementary data to this article can be found online at https://doi.org/10.1016/j.cretres.2022.105315.

UNCORRECTED PROOF